Gamma-ray spectrometry in the field: radioactive heat production in the Central Slovakian Volcanic Zone

Thomas L. Harley[1,2], **Rob Westaway**[1,3] and **Alistair T. McCay**[1]

[1] School of Engineering, University of Glasgow, James Watt (South) Building, Glasgow G12 8QQ, U.K.
[2] Present address: WSP - Parsons Brinckerhoff, 6 Devonshire Square, London EC2M 4YE, U.K.
[3] Corresponding author; email: robert.westaway@glasgow.ac.uk

Abstract

We report 62 sets of measurements from central-southern Slovakia, obtained using a modern portable gamma-ray spectrometer, which reveal the radioactive heat production in intrusive and extrusive igneous rocks of the Late Cenozoic Central Slovakian Volcanic Zone. Sites in granodiorite of the Štiavnica pluton are thus shown to have heat production in the range ~2.2-4.9 μW m^{-3}, this variability being primarily a reflection of variations in content of the trace element uranium. Sites in dioritic parts of this pluton have a lower, but overlapping, range of values, ~2.1-4.4 μW m^{-3}. Sites that have been interpreted in adjoining minor dioritic intrusions of similar age have heat production in the range ~1.4-3.3 μW m^{-3}. The main Štiavnica pluton has zoned composition, with potassium and uranium content and radioactive heat production typically increasing inward from its margins, reflecting variations observed in other granodioritic plutons elsewhere. It is indeed possible that the adjoining dioritic rocks, hitherto assigned to other minor intrusions of similar age, located around the periphery of the Štiavnica pluton, in reality provide further evidence for zonation of the same pluton. The vicinity of this pluton is associated with surface heat flow ~40 mW m^{-2} above the regional background. On the basis of our heat production measurements, we thus infer that the pluton has a substantial vertical extent, our preferred estimate for the scale depth for its downward decrease in radioactive heat production being ~8 km. Nonetheless, this pluton lacks any significant negative Bouguer gravity anomaly. We attribute this to the effect of the surrounding volcanic caldera, filled with relatively low-density lavas, 'masking' the pluton's own gravity anomaly. We envisage that emplacement occurred when the pluton was much hotter, and thus of lower density, than at present, its continued uplift, evident from the local geomorphology, being the isostatic consequence of localized erosion. The heat production in this intrusion evidently plays a significant role, hitherto unrecognized, in the regional geothermics.

Key words: Slovakia, Miocene, Štiavnica pluton, heat flow, heat production, gamma-ray spectrometry

Highlights:

Igneous rocks emplaced during Miocene subduction are abundant in central Slovakia
A modern field-portable gamma-ray spectrometer has been used to study these rocks
The largest igneous complex includes the compositionally-zoned Štiavnica pluton
Heat production in this granodiorite reaches 5 μW m^{-3}, mainly due to uranium content
To account for the observed heat flow anomaly requires this pluton to be ~8 km thick

1…Introduction

Central-southern Slovakia (Fig. 1) was affected by widespread magmatism, involving both extrusive volcanism and the emplacement of granitic intrusions, during subduction along the Carpathian arc in the Middle Miocene (Fig. 2), forming the Central Slovakian Volcanic Zone (CSVZ) (Fig. 3). The surface heat flow in this region (Tables 1 and 2; Fig. 4) is high enough for thermal groundwater to be a significant local

resource for thermal spas and water parks and most recently for an incipient geothermal energy industry. However, at present only limited understanding exists regarding the causal mechanism for this resource. As part of a multi-disciplinary study of this significant region, we have carried out an initial survey of radioactive heat production in its rocks, using a portable gamma ray spectrometer of modern design ('Gamma Surveyor II'; GF Instruments S.R.O., Brno, Czech Republic; for details see, e.g., www.gfinstruments.cz/version_cz/downloads/GMS_II.pdf). Relatively little has been published on the results obtainable by use of modern equipment of this type, which offers several advantages, in terms of data quality and ease of use, over older equipment based on similar principles, which came into use decades ago (see below). We are not aware of any previous work of this type in the present study region, although Lexa et al. (1999) summarized airborne gamma ray spectrometry results in part of the region.

Figure 1 here: location map
Figure 2 here: Map of the Carpathian Arc and Pannonian Basin
Figure 3 here: Map of Miocene volcanism
Table 1 here: Summary of heat flow results from Cermak (1979)
Table 2 here: Summary of heat flow results from Franko et al. (1995)
Figure 4 here: heat flow map

We shall first summarize relevant background information on the study region. We shall then explain the technique used in the field and present the results obtained by using it. We conclude by discussing the implications of these results for the geothermics of the study region, addressing the zoned composition and vertical extent of the studied igneous bodies.

2…Background on the study region

The continental crust of Slovakia, forming part of the modern ALCaPa (Alpine-Carpathian-Pannonian) block (Fig. 2), has had a long and complex tectonic history. Distinct crustal provinces, or terranes, which experienced independent histories of plate motion during the Palaeozoic, have been recognized within this block (e.g., Plašienka et al., 1997). In general terms, the crust now forming this region is thought to have rifted from Gondwana during the Lower Palaeozoic and accreted against the ancestral Eurasian continent, Laurussia, during the Variscan orogeny. It separated from this continent in the early Mesozoic as a result of the opening of the Ligurian-Piemont ocean, or rather its eastern continuation known as the Vahic-Pieniny ocean, becoming part of the Apulian continent (also known as Adria) within the Neotehyan realm. The subsequent (Late Cretaceous and Cenozoic) convergence between Africa and Eurasia initially involved subduction of the Ligurian-Piemont-Vahic-Pieniny ocean beneath Apulia / Adria. By the Oligocene, when the continental collision between Africa and Eurasia began in the central Alpine region, a remnant of the former ocean, known as the Carpathian Embayment or 'Carpathian Ocean', persisted farther east. Continued convergence between Africa and Eurasia was accommodated by right-lateral strike-slip faulting on the west-east-trending Peri-Adriatic Fault Zone and its eastern continuation, the Mid-Hungarian Fault Zone, accompanying eastward extrusion of the continental crust, derived from Apulia / Adria, forming the Austroalpine zone of the Alps and its eastward continuation, the AlCaPa block, to the north of this fault zone (Fig. 2). This eastward movement was accommodated by subduction of the Carpathian Ocean beneath the AlCaPa block, which itself resulted in eastward extension (i.e., 'backarc extension'), creating the extensional Pannonian Basin that is mostly located in Hungary but continues northward into southern Slovakia, and also causing the subduction-related magmatism in the CSVZ. Further details beyond this summary account are provided in a copious literature (e.g., Stegena et al., 1975; Royden et al., 1983; Szabo et al., 1992; Plašienka et al., 1997; Szafián et al., 1997; Konečný et al., 1999; Stampfli et al., 2001, 2002; Von Raumer et al., 2002, 2003; Bielik et al., 2004; Schmid et al., 2004; Alasonati-Tašárová et al., 2009; Handy et al., 2014; Broska and Petrík, 2015; Horváth et al., 2015). The

formerly distinct crustal provinces or terranes, which sutured together before and during the Variscan orogeny to form the modern AlCaPa block, include the Tatra-Fatra Belt and the Vepor Belt (e.g., Plašienka et al., 1997). Figure 5 depicts a summary Bouguer gravity anomaly map for a swathe through this region. It is thus apparent that the principal gravity effect is the north-south increase in Bouguer anomaly. Many workers (e.g., Bielik et al., 1991; Bielik, 1999; Alasonati-Tašárová et al., 2009) have explained this as a consequence of the transition from thickened crust in the Carpathian Mountains to the north to thinned crust in the centre of the Pannonian Basin to the south, as a result of the Cenozoic plate-tectonic processes summarized above (cf. Fig. 2), the principal contributing factor being the southward decrease in Moho depth. Superimposed onto this regional-scale effect are more localized anomaly patters including variations associated with the Štiavnica and Javorie uplands. We will present a summary analysis of these patterns in relation to the structure and thermal state of these uplands (see below, section 5.4).

Figure 5 here: regional gravity anomaly map

Many workers have reported background information on the regional geothermics of Slovakia, including heat flow measurements, maps of surface heat flow, and modelling to determine temperatures at depth (e.g., Boldizsár, 1964; Lizoň, 1975; Čermák, 1977, 1979; Bielek et al., 1991, 2010; Franko et al., 1995; Zeyen et al., 2002; Dérerová et al., 2006). The works on subsurface temperature modelling have evidently incorporated the effect of radioactive heat production in different crustal layers, but have not made clear what values they used or on what measurements they are based; in some cases, inaccessible unpublished documents are cited, which presumably contain this information. The initial starting point for the present analysis was the accessible Čermák (1979) publication, which documented all geothermal data then available from the present study region (Table 1), including a heat flow measurement in the Banská Štiavnica area, from the Klinger Kratka mine (Fig. 6(a)), thus demonstrating the local high heat flow that the present analysis seeks to explain. We also consulted the less accessible 'Atlas of Geothermal Energy in Slovakia' by Franko et al. (1995). This reports a much denser network of subsurface temperature and heat flow measurements (Table 2; Fig. 6(b)), from which modern maps of surface heat flow (such as that in Fig. 4) confirm the local heat flow 'high' around Banská Štiavnica, ~40 mW m^{-2} above the regional 'background'. We note, nonetheless, that there are many discrepancies between these two data sources (e.g., those listed in Table 1), resolution of which is beyond the scope of the present study.

Figure 6 here: local details

The principal research targets of this study are the Middle Miocene igneous rocks forming the aforementioned Štiavnica and Javorie uplands (Figs. 3, 6). Covering a ~2200 km^2 area, the igneous complex emplaced by the 'Štiavnica Stratovolcano' is the largest to have developed as a result of the Late Cenozoic subduction along the Carpathian arc. The structure and stratigraphy of this igneous complex were established in many works in the local literature (e.g., Konečný and Lexa, 2001), an accessible summary in English aligned with a quantitative chronology having been provided by Chernyshev et al. (2013). At a late stage in this subduction-related magmatism, the rocks experienced pervasive hydrothermal activity associated with metalliferous mineralization, primarily for silver but also including gold (e.g., Bauer, 1999; Bahna and Chovan, 2001; Kodera et al., 2001, 2004, 2014; Bella et al., 2010, 2016). This region, in particular the surroundings to the medieval town of Banská Štiavnica, indeed formed one of the principal sources of precious metals in Europe for many centuries (e.g., Valderrama and Pérez-Pariente, 2012; Herčko et al., 2014; Karsten, 2015). As a result of this history, including the region's contribution to the industrial revolution, it has been designated as a World Heritage Site (UNESCO, 1993). In contrast, the present-day local economy depends largely on tourism (e.g., Darulová, 2010), including the utilization of thermal water in spas (e.g., Fričovský et al., 2016). Like the mining, some of the region's thermal spas are

of some antiquity, those in the villages of Vyhne and Sklené Teplice dating back to the 16th century (e.g., Fendek et al., 1999). Extraction of thermal waters as sources of geothermal energy is also envisaged (e.g., Remšík et al. (2009). The need to understand the underlying geothermics, to inform geothermal developments in this sensitive region, has motivated the present study; as Fendek and Fendeková (2015) have noted, abstraction of thermal waters in Slovakia is tightly regulated, with a legal obligation on operators to use resources sustainably.

As regards the potential significance of geothermal energy in this area, Remšík et al. (2000, 2001) estimated its exploitable geothermal resource as ~9.5 MW, comprising the thermal waters at temperatures of 32-53 °C, used at the Vyhne and Sklené Teplice thermal spas, and other waters being drawn from boreholes or flowing from drainage adits constructed to dewater now-disused mine workings (Fig. 6(a)). Remšík et al. (2009) revised this estimate upward to ~22.3 MW but interpreted the most important geothermal resource to the north of the Štiavnica upland around Žiar nad Hronom (Fig. 1). However, none of these studies even mentioned the Štiavnica pluton (Fig. B) as a potential contributor to the geothermal resource. Bajtoš (2001) inventoried additional contributions to this resource, omitted from the aforementioned inventories, from warm water flowing out of other mine drainage adits, totalling ~5.3 MW; these include the discharge from the Voznícka adit in the Hron valley, ~5 km west of Hodruša-Hámre (Fig. 6(a)). The total of resources and reserves (including 'probable reserves') of geothermal heat in Slovakia was estimated initially as ~5.5 GW (e.g., Fendek and Fendeková, 2005; Pavolová et al., 2010), then as ~6.7 GW (Fendek et al., 2011; Fričovský et al., 2012), suggesting that further investigations might identify further resource potential. More recently, Černák et al. (2014) revised this estimate downward to ~6.2 GW, although still without recognition of heat production in granitic plutons.

The Štiavnica upland covers a ~30 km by ~30 km area, centred around Banská Štiavnica. Its highest point is the summit of the mountain Sitno, ~6 km south of this historic town, reaching 1009 m above sea-level, with many other summits between 800 and 900 m. The western half of this upland is drained by several short rivers, which flow westward into the River Hron along deeply entrenched valleys; these include the Hodrušsky Potok, which joins the Hron at Žarnovica (Figs 1, 6(a)). The Hron is one of the principal left-bank tributaries of the Danube, with a confluence at Šturovo (Fig. 1); it falls from ~240 m above sea-level at Žiar nad Hronom to 214 m at Žarnovica and ~195 m at Nová Baňa. The less rugged eastern part of the upland drains southward via the River Štiavnica and its tributaries (Fig. 6(a)). The Štiavnica joins the Ipeľ near Šahy (Fig. 1); the latter river, another major Danube tributary, continues southward, delineating the Slovakia-Hungary border, to its confluence with the Danube downstream of Šturovo.

The Late Cenozoic stratigraphy of this region is referenced to that of the landlocked Paratethys 'sea', the chronology of which has proved most difficult to quantify (cf. Rögl, 1996; Steininger and Wessely, 2000; Piller et al., 2007; Vasiliev et al., 2010). For example, in the Piller et al. (2007) scheme, the Badenian stage spans ~16.0 Ma to ~12.4 Ma, the Sarmatian ~12.4 to ~11.6 Ma, the Pannonian ~11.6 to ~6.0 Ma, and the Pontian ~6.0 Ma to the end of the Miocene at ~5.4 Ma. According to Chernyshev et al. (2013), development of the 'Štiavnica Stratovolcano' occurred in five stages (Fig. 3), during the Early Badenian to earliest Pannonian stages of this timescale. First, an extensive andesitic stratovolcano developed during 15.0-13.5 Ma. Erosion of this volcanic edifice was followed, between 13.5 and 12.9 Ma, by the initial subsidence of the associated caldera and the contemporaneous emplacement of an intrusive complex, including granodiorite and diorite intrusions. The third phase, subsidence of the caldera and its infilling with differentiated andesite during 13.1-12.7 Ma, overlapped with the youngest intrusive activity. Renewed explosive and effusive eruption of less differentiated andesite spanned 12.7-12.2 Ma, and was followed, according to Chernyshev et al. (2013), by uplift of the 'resurgent horst' at the centre of the caldera, accompanied during 12.2-11.4 Ma by rhyolitic volcanic/intrusive activity. In their view the

hydrothermal ore mineralization was contemporaneous with this phase and continued until 10.7 Ma. Support for this chronology was provided by K-Ar dating to 12.0-10.7 Ma of the gangue mineral adularia in hydrothermal veins. Adularia is a low-temperature crystal form of potassium feldspar, the highest-temperature type of which crystallizes circa 254-287 °C (Dong and Morrison, 1995). Rapid cooling is thus indicated in the circa two million years following the intrusion of the granodiorite, at an estimated temperature of 750 °C (Nemčok et al., 2000).

Figure 4 illustrates a small part of the Pannonian-Carpathian region, across which heat flow increases southward on a regional scale from ~50-60 mW m^{-2} in central-southern Poland to ~120 mW m^{-2} in Hungary (e.g., Dérerová et al., 2006), this latter locality being where the Miocene crustal extension and thinning in the Pannonian Basin was concentrated (Fig. 2). In much of the area of Fig. 4 the surface heat flow is ~70 mW m^{-2}, a value that we take as the 'regional background' for this part of the Pannonian-Carpathian region. Figure 4 and the supporting data in Tables 1 and 2 show that the surface heat flow is ~110 mW m^{-2} at the centre of the Štiavnica pluton, thus ~40 mW m^{-2} higher than the regional background. Surface heat flow indeed decreases to the ~70 mW m^{-2} regional background to the west, north and east of this pluton. Circa 50 km south of the Štiavnica pluton, a ~30 km wide east-west-trending zone of higher heat flow, up to ~90 mW m^{-2}, is evident. However, the nature of this zone, including the cause of its ~20 mW m^{-2} heat flow anomaly relative to the regional background, is beyond the scope of the present study. The ~70 mW m^{-2} regional background heat flow is evidently the result of the combination of processes, documented above, affecting the study region during its complicated geological history. Determining how each of these processes might have influenced this background heat flow is another topic that is beyond the scope of the present study; our interest is in trying to understand the cause of the ~40 mW m^{-2} higher heat flow at the centre of the Štiavnica pluton.

We note in passing that one of the most accessible summary descriptions of this study region, by Drew (2006), interprets the Štiavnica upland as a graben or pull-apart basin that developed at a leftward step in SW-NE-oriented left-lateral strike-slip faulting. The pull-apart basin that is interpreted in this scheme corresponds to the 'resurgent horst' at the centre of the Štiavnica caldera (compare Fig. 37 of Drew, 2006, with Fig. 3), indicating the opposite polarity of the component of normal slip on the faults bounding this structure. We are unconvinced regarding this interpretation and prefer to base our investigations on the local literature.

Petrological and geochemical classifications of the CSVZ igneous rocks have been presented in many studies (e.g., Harangi et al., 2007; Seghedi and Downes, 2011; Chernyshev et al., 2013) so only brief details are repeated here; a summary classification of the rocks that we have investigated is provided in Fig. 8(a), with greater detail for the Štiavnica upland in Fig. 9(a). Beyond this, and the summary depictions of the geology in Figs 3, 6(a) and 7, no attempt is made in the present study to depict the complexity of this region in map form; such detail is covered in local publications, such as that by Chernyshev et al. (2013), and in the online geological map dataset for Slovakia (available at http://mapserver.geology.sk/gm50js/, with maps at scales of up to 1:10,000). However, we also note in passing that major differences exist between this mapping, on which our fieldwork was based, and the Chernyshev et al. (2013) interpretation. For example, the geological map depicts the intrusive phase as Badenian-Sarmatian whereas the Chernyshev et al. (2013) scheme places it (their phase 2) entirely within the Badenian. Second, some of the lithological descriptions differ, for example, Chernyshev et al. (2013) interpret some of their minor 'phase 2' intrusions as consisting of 'granodiorite' and/or 'quartz-diorite porphyry' whereas the geological map shows rocks of andesitic composition in the same places. Third, the age order of much of the succession has been modified; in particular, much of the lava that is portrayed on the geological map as Late Badenian, making it older than the 'Badenian-Sarmatian' intrusive phase, is assigned by Chernyshev

et al. (2013) to their phase 3, making it younger than this intrusive phase. Chernyshev et al. (2013) also introduced new terminology: they named the main pluton in the Štiavnica upland (Fig. 3) as the 'Hodruša-Štiavnica Intrusive Complex' and designated the 'Zlatno Intrusive Complex' in the north (near Sklené Teplice) and the 'Tatiar Intrusive Complex' in the south (near Pukanec) while also grouping the widespread sill intrusions throughout the upland as the 'Banisko Intrusive Complex'. Since Chernyshev et al. (2013) reported the 'Zlatno' and 'Tatiar' intrusive complexes as consisting in part of granodiorite, and thus potentially significantly radiothermal, they became targets for our research, even though (as noted above) the geological map shows only andesite cropping out in these localities. To briefly summarize this very complicated story, the central part of the Štiavnica upland is interpreted as the uplifted 'resurgent horst' of ~10-15 km diameter, underlain by the Štiavnica pluton (its top ~800 m above sea-level), at the centre of the ~20 km diameter caldera (Figs. 3 and 7). Chernyshev et al. (2013) produced a schematic cross-section through this pluton with its base at roughly the same level in the landscape as the Hron valley, implying that the granodiorite is no more than a few hundred metres thick. However, granodiorite is directly documented to a depth of ~2000 m below the top of the pluton, from mine records and associated borings (e.g., Lexa et al., 1999; Nemčok et al., 2000; Chernyshev et al., 2013). The gentle outward slope of the 'dome-shaped' top of this pluton is also depicted in published cross-sections based on mining records (e.g., Lexa et al., 1999; Nemčok et al., 2000; Chernyshev et al., 2013). Nemčok et al. (2000) envisaged the pluton as cylindrical with a 10 km diameter and a 7 km vertical extent, its top emplaced at ~2.5 km depth. The gently outward sloping 'dome-shaped' top of this pluton is depicted in published cross-sections based on mining records (e.g., Lexa et al., 1999; Nemčok et al., 2000; Chernyshev et al., 2013). We later revisit the question of the thickness of this pluton (sections 5.3 and 5.4).

Figure 7 here: Map showing sites in relation to outcrop of the Štiavnica pluton
Figure 8 here: Map of results for whole region
Figure 9 here: Map of results for central part of region

A phase of basaltic andesite volcanism is thought to date from ~10-8 Ma, being represented by necks such as Šibeničný Vrch adjoining the Hron valley east of Žiar nad Hronom (Fig. 3; e.g., Šimon et al., 2002a). Subsequent alkali basaltic volcanism near Banská Štiavnica is revealed by the Kalvária and Kyhisýbel necks (Fig. 3), dated by Chernyshev et al. (2013) to ~7.3 and 7.8-7.2 Ma. However, any basalt flows that erupted from these necks have since been lost to erosion, indicating that denudation by (? many) hundreds of metres has occurred locally, in this part of the caldera outside the 'resurgent horst', since these eruptions. Rapid denudation is also implied by the narrowness (in relation to depth) of river valleys draining this magmatic centre, such as those of the Vyhniansky Potok and the aforementioned Hodrušsky Potok (Fig. 6(a)), and is consistent with a substantial uplift rate in the vicinity (cf. Binnie et al., 2007; Hurst et al., 2013). Uplift can be expected as an isostatic consequence of intrusion of granitic rock of lower density than its surroundings. It can also be anticipated as the isostatic response to such denudation, making it improbable that uplift of the Štiavnica upland ended in the Middle Miocene as Chernyshev et al. (2013) have proposed. In contrast, other alkali basaltic volcanoes of similar age in surrounding regions do not show comparable evidence of erosion, necks being associated with extensive outcrop of basalt flows (e.g., Konečný et al., 1999), indicating that the rapid denudation and associated uplift within the Štiavnica upland have been quite localized.

Finally, on the western flank of the upland there is a single (?) Middle Pleistocene basalt flow unit, which erupted from the Pútikov Vršok neck and flowed into the Hron valley at Brehy near Nová Baňa (e.g., Konečný et al., 1999; Chernyshev et al., 2013). A range of ages within the Middle Pleistocene has been proposed for this eruption (e.g., Konečný et al., 1999; Šimon et al., 2002b; Chernyshev et al., 2013). This basalt covers part of a low terrace of the Hron, of inferred 'Riss-Würm' age according to Konečný et al.

(1999) or 'Riss' age according to Šimon et al. (2002b), ~10 m above the modern river. Higher spreads of fluvial sand and gravel, up to ~180 m above this river, have also been mapped in its reach between Žiar nad Hronom and Nová Baňa, and evidently indicate a substantial Hron terrace staircase. Although the geological map assigns these deposits a notional Pliocene age (they are labelled as bbPl; banskobystrické súvrstvie, meaning 'Banská Bystrica Formation' of 'Pliocene' age), a succession of ages associated with cyclic variations in Pleistocene climate would be more in keeping with modern ideas regarding fluvial terrace development (e.g., Bridgland, 2000; Bridgland and Westaway, 2008a, 2008b). Farther downstream, in the ~50 km lowland reach of the lower Hron between Levice and its Danube confluence at Štúrovo, Šujan and Rybár (2014) have recognized a staircase of six fluvial terraces, the highest ~80 m above the modern river. They assumed that this oldest terrace formed around the start of the Pleistocene (~2.6 Ma) and thus inferred an uplift rate of ~0.03 mm a^{-1}. Another possibility (cf. Bridgland, 2000) is that these terraces might represent successive 100 kyr climate cycles, in which case the oldest recognized dates back to MIS 14 and the uplift rate has been ~0.15 mm a^{-1}. It is unclear at this stage whether the presence of fluvial terraces to a much greater height within the landscape in the middle Hron between Žiar nad Hronom and Nová Baňa indicates faster uplift or greater antiquity of the oldest terraces than in the lower Hron; the deeply-entrenched character of the aforementioned Hron tributaries draining the Štiavnica upland nonetheless suggests a substantial uplift rate in the vicinity (cf. Binnie et al., 2007; Hurst et al., 2013).

3…Fieldwork and data analysis

Field measurements were made using a 'Gamma Surveyor II' portable gamma-ray spectrometer (GF Instruments S.R.O., Brno, Czech Republic; e.g., www.gfinstruments.cz/version_cz/downloads/GMS_II.pdf), which uses the gamma radiation emitted by the radionuclides responsible for radioactive heat production to estimate their concentrations. It passively detects, using a bismuth germanate ($Bi_4(GeO_4)_3$; also known as 'bismuth germanium oxide' or BGO) scintillation crystal, this radiation at 1024 frequencies between 30 keV and 3 MeV, which encompass the spectrum of gamma-ray photons emitted by radioactive decay of the heat-producing isotopes of potassium (K), uranium (U), and thorium (Th). The calibration (which is carried out by the manufacturer in accordance with International Atomic Energy Agency procedures; e.g., IAEA, 2010) assumes that the gamma radiation is incident on the detector from throughout a solid angle of 2π steradians, consistent with placement on a planar rock surface. Subject to this assumption, the manufacturer's documentation reports measurement accuracies of ±0.14 wt% for potassium, ±0.8 ppm for uranium (U), and ±1.5 ppm for thorium (Th), for a standard measurement run of three minutes duration on a typical low-radioactivity sample (i.e., 2.3±0.14 wt% K, 2.7±0.8 ppm U, 9.4±1.5 ppm Th, giving percentage uncertainties for this sample of ~6%, ~30%, and ~16%, respectively). As McCay et al. (2014) discussed, a portable detector of this type, operated in this manner, will effectively sample gamma-ray photons emitted by a ~0.15 m deep by ~1.0 m diameter disc of rock below the rock surface; field sites were selected with this criterion in mind. Wherever possible, measurements were made on recently-exposed rock surfaces, typically in road cuttings or quarry faces, to avoid systematic errors caused by surficial rock weathering, which can result in leaching or uptake of water-soluble radionuclides. Wherever possible, the measurements were made on flat surfaces with dimensions of >2 m, at points >1 m from the edges of the exposure, to avoid systematic errors resulting from the rock mass subtending a solid angle significantly different from 2π steradians. McCay et al. (2014) have provided a more detailed account of the physical principles and operational procedure of this type of equipment, details that are therefore omitted here. IAEA (2003) also provides extensive background information on the physics underlying gamma-ray spectrometry, although this report pre-dates the development of modern field equipment including that which we have used (see, also, below). Portable gamma-ray spectrometers were already in use in the field in the 1980s (e.g., Feely and Madden, 1987) but suffered from a number of problems (e.g., Løvborg, 1984). They typically only

recorded gamma rays at four frequencies, rather than across the spectrum. Furthermore, the alkali metal halide (typically, sodium iodide) scintillation detectors then in use had limited frequency resolution and also experienced 'drift' of the frequencies detected, making them prone to significant systematic error. In addition, this scintillator material was relatively insensitive, so the detectors had to be made rather large to avoid long measurement times. One, nonetheless, occasionally sees publications reporting continued use of this older generation of equipment (e.g., Attia and Wahid, 2016).

As already noted, the Gamma Surveyor II records across the gamma-ray spectrum, eliminating the issue of systematic error resulting from limited frequency resolution. Furthermore, BGO, the scintillator used, is an optimal material for several reasons (e.g., http://www.kinheng-crystal.com/products-detail.asp?id=1340). In particular, the high atomic number of bismuth facilitates absorption of gamma-ray photons, increasing the sensitivity, making it possible for a BGO detector to be a tenth of the size of a sodium iodide detector of equivalent performance. This is reflected in the small size of the instrument, evident from comparison of illustrations in the manufacturer's documentation (e.g., www.gfinstruments.cz/version_cz/downloads/GMS_II.pdf) with those of the much larger apparatus formerly in use (e.g., Fig. 1 of Løvborg, 1984); the logistics of fieldwork benefit significantly from this.

As Šefara and Bielik (2009) have noted, an extensive investigation programme, involving ~4000 sets of measurements of radioactive heat production, took place in Slovakia in the 1980s. Results of this work have been summarized by Husák and Král (1984, 1986) but the dataset thus produced has never been published. However, given the difficulties associated with equipment of this era (described above), we have not attempted to consult this historic dataset in any archive in Slovakia, for comparison with our own results. Other than an airborne gamma spectrometry survey reported by Lexa et al. (1999), which is briefly discussed below, we are unaware of any more recent work of this type in any locality that we have investigated.

The Gamma Surveyor II can be connected to a portable GPS receiver to electronically log the position of each site as well as the measurement results. However, since the steep rock surfaces typically selected for measurement block the signals from GPS satellites, it proved more effective to measure position using a separate handheld GPS receiver that could be taken to nearby localities with better sky visibility while the spectrometer was measuring. These co-ordinates were thus written in a notebook, rather than logged electronically, along with the numerical outputs of the gamma ray spectrometer. Following the fieldwork, the spectrometer's internal files containing the measurement results were downloaded and these numerical results were merged with the site co-ordinates into a spreadsheet. Rock samples were also collected at most sites, to confirm (or, occasionally, amend; see below) in the laboratory the mapped stratigraphic interpretations; the aforementioned http://mapserver.geology.sk/gm50js/ online geological mapping was used for site selection and for these comparisons.

The convention was adopted of recording field site co-ordinates from the handheld GPS receiver using the Universal Transverse Mercator (UTM) / Military Grid Reference System (MGRS) notation. Co-ordinates thus expressed can be readily converted into geographical co-ordinates if required, using online calculators such as that by Earthpoint (http://www.earthpoint.us/Convert.aspx), so that latter are not reported in the present study. However, large-scale topographic maps and other facilities in Slovakia, such as the online geological map, use a different co-ordinate system, based on the Křovák projection. As Veverka (2004) has explained, this was devised in 1922 by the geodesist Josef Křovák to enable a grid of maps to be prepared that minimized the effects of angular distortion and length distortion for the newly-created country of Czechoslovakia that (with its original 1919 borders) was >900 km long in the WNW-ESE direction but typically <200 km wide. The origin of the Křovák co-ordinate system is near Talinn in Estonia,

due north of the eastern end of the former Czechoslovakia; as a result, X- and Y-co-ordinates in this system are both negative in modern Slovakia, with the X-axis oriented roughly ESE and the Y-axis roughly NNE. Co-ordinates in this system were essential to locate ourselves in the field on both topographic and geological maps; we used the Majster V1.1 spreadsheet by Gábor Timár (available online: http://sas2.elte.hu/tg/majster.xls) to convert between them and UTM co-ordinates.

Radioactive heat production, Y, was calculated from the measured radionuclide concentrations using the formula

$$Y = \rho (0.03476\, C_K + 0.09528\, C_U + 0.02561\, C_{Th}) \quad (1)$$

from Rybach (1976), converted into S.I. units. Here, ρ is the density of the rock and C_K, C_U, and C_{Th} are the concentrations of the three radionuclides measured (in units of wt% for K and ppm for U and Th). Using these units and with the numerical constants as stated, this formula gives Y in nW m^{-3}. For the present analysis, a nominal density of 2700 kg m^{-3} has been adopted for all rock types. For each site, the results from three three-minute spectrometer measurements on adjacent rock surfaces (not at precisely the same place) were averaged together. Given the typical distances travelled by the gamma-ray photons (see above) and our measurement and analysis procedures, we thus obtained overall values for the radionuclide concentrations and the associated heat production that are each representative of ~0.4 m^3 or ~1000 kg of rock, much larger samples than could conceivably be returned for analysis in the laboratory. This use of a nominal density value introduces uncertainties into the measured Y values. However, it would evidently have defeated the point of taking a portable measuring device into the field if we had returned large rock samples from each site to permit accurate measurement of density. The nominal value of 2700 kg m^{-3} used is likely to approximate the actual density of the granodiorite samples analysed; for example, Rybach and Buntebach (1981) estimated the typical density of granodiorite as 2700 kg m^{-3}, whereas Tenzer et al. (2011) reported 2681$\pm$70 kg m^{-3} ($\pm 1\sigma$). However, it probably overestimates the density of the andesite samples whose actual density, reported by Remšík et al. (2001), is quite variable, in the range 2300-2540 kg m^{-3} with a typical value of ~2470 kg m^{-3}. On the other hand, the diorite samples probably had somewhat higher density; Rybach and Buntebach (1981) estimated a typical value of 2840 kg m^{-3}, whereas Tenzer et al. (2011) reported 2797$\pm$119 kg m^{-3} ($\pm 1\sigma$). The basalt samples analysed probably likewise have higher densities, maybe ~2900 kg m^{-3} (Tenzer et al., 2011, reported 2768$\pm$162 kg m^{-3}, $\pm 1\sigma$). On this basis it can be inferred that our estimates of Y may typically be ~9% too high for the andesites and ~7% too low for the basalts; these margins are comparable to the variability observed between the replicate measurements at many sites and much less than the observed variations between lithologies.

We emphasize that the parameter C_K in equation (1) is the percentage by weight of potassium (e.g., IAEA, 2003, p. 16). However, it is customary in geochemistry to express concentrations of major elements as the percentage by weight of their oxides, in this case K_2O. Since the molar masses are 39.098 g for potassium and 94.196 g for K_2O, this compound is 83.014% potassium by weight. One must therefore incorporate this numerical factor when comparing measurements of potassium content obtained using a gamma-ray spectrometer with the results of geochemical analyses (expressed conventionally) for the same rock.

4…Results

Table 3 summarizes the outcome of our analysis, a full table of results being provided in the online supplement. Figure 8(b) illustrates the geographical distribution of radioactive heat production values across the study region, with an enlargement of the results in the immediate vicinity of Banská Štiavnica

in Fig. 9(b); site locations in relation to the mapped outcrop of the Štiavnica pluton are depicted in Fig. 7. To place these results in context, granitic rocks with heat production >4 μW m^{-3} are generally regarded as potential geothermal resources (e.g., McCay et al. 2014). The results will now be discussed, grouped by lithology.

Table 3 here: Table of heat production results

4.1 Basement rocks

We sampled the (pre-) Variscan crystalline basement or 'Kryštalinikum' at two sites beyond the northern and eastern margins of the Štiavnica upland, in a cutting on the recently-widened Zvolen-Lučenec highway at Podkriváň, to the east (site 28 in Fig. 8(a)), and in the disused quarry at Lieskovec, to the northeast (east of Zvolen; site 61). The granodiorite sampled at both these sites had low heat production, in the range ~1-2 μW m^{-3} (Table 3). Small inliers of 'Kryštalinikum' are also mapped within the Štiavnica upland (Figs. 3, 6(a)), but these proved difficult to find due to pervasive forest vegetation. Several exposures of granitic schist were nonetheless identified along the Vyhniansky Potok valley between Vyhne and Banky (sites 40, 41 and 43 in Fig. 9(a)), the 'hottest' of which (site 41; Table 3) had heat production ~3.6 μW m^{-3}. In terms of basement structure (e.g., Hrouda et al., 2002) the Podkriváň site falls within the principal outcrop of Vepor Belt basement, the Lučenec outcrop is an inlier of Vepor Belt basement, and the Štiavnica upland sites fall within the Tatra-Fatra Belt basement. Since these two groups of sites are located within what were, prior to the Variscan Orogeny, distinct crustal provinces (e.g., Plašienka et al., 1997), differences in composition, which cause the observed differences in heat production, are not surprising.

4.2 Post-orogenic alkali basalts

Many small basaltic outcrops, forming lava flows or volcanic necks, are mapped in the Banská Štiavnica area and its surroundings, which represent eruptive activity between the latest Miocene (~8 Ma) and the Middle Pleistocene (e.g., Konečný et al., 1999; Chernyshev et al., 2013; Fig. 3). We measured the heat production at four sites in basalt flows of nominal 'Pontian' (i.e., latest Miocene) age, at Ostrá Lúka (near Zvolen; site 26 in Fig. 8(a)), Podrečany (near Lučenec; site 29), Rakovec (near Krupina; also known as the Devičie basalt; site 30), and Mochovce (west of Levice; site 62), which are classified on the geological map as nepheline basanites. We also sampled the youngest basalt flow in the region, from the aforementioned Putikov Vršok neck near Nová Baňa (site 17 in Fig. 8(a)), which is classified on the map as nepheline tephrite. These basalts appeared quite different in hand specimen: those from Ostrá Lúka and Rakovec contained plagioclase phenocrysts up to ~3 mm in size, although at the former site these were unweathered whereas at the latter they showed signs of kaolinization; that from Mochovce contained phenocrysts of both plagioclase and augite, both up to ~3 mm in size; whereas the basalts from Podrečany and Brehy consisted entirely of microcrystalline groundmass. Chernyshev et al. (2013) presented major element geochemical analyses (e.g., 45-48% SiO_2; 1.3-1.9% K_2O) and summary petrographic descriptions of a set of samples of these alkali basalts. Notwithstanding the evident compositional differences, the site measurements all indicate low heat production, in the range ~1-2 μW m^{-3} (Table 3).

4.3 Javorie 'argillite'

We attempted to investigate the dioritic rocks of the Javorie intrusive complex, which the geological map shows cropping out over several square kilometres in the centre of the Javorie upland around Vigľašská Huta – Kalinka, but could find no exposure. However, we sampled an outcrop of 'argillite' that the map depicts as directly overlying this intrusion (site 27 in Fig. 8(a)). In local usage (e.g., Kodera et al., 2001) 'argillite' denotes a rock that has been reduced essentially to clay minerals as a result of hydrothermal alteration due to close proximity of an igneous intrusion. The material at Vigľašská Huta – Kalinka, thus named, consisted of indurated white rock, with a powdery weathered groundmass,

presumably derived from hydrothermal alteration of plagioclase to clay minerals, which could be seen (on examination in hand specimen) to preserve small crystals (up to ~1 mm) of augite and biotite. Relatively high heat production, ~3.2 $\mu W\ m^{-3}$, was measured (Table 3).

4.4 Štiavnica granodiorite / diorite pluton

The Middle Miocene Štiavnica pluton (the 'Hodruša-Štiavnica Intrusive Complex' of Chernyshev et al., 2013; Fig. 3) has a mapped extent (Fig. 7) of ~8 km east-west (from Hodruša-Hámre to Banky) and ~5 km north-south (from Vyhne to Kopanice). According to Kodera et al. (2004, 2014) the top of this pluton slopes outward at a typical angle of ~30°, making it more extensive in the subsurface than its small area of outcrop would appear to imply; at depth it presumably approximates the full extent of the Štiavnica 'resurgent horst' (Fig. 3). Its form has also been affected by the throw on many normal faults, creating multiple localities with the pluton cropping out in footwalls but country rock in hanging-walls.

This pluton is mapped as dioritic in the northeast; Chernyshev et al. (2013) presented a major element geochemical analysis (e.g., 56% SiO_2; 1.5% K_2O) and a summary petrographic description for a single sample, consisting of plagioclase in the compositional range 55-72% anorthite (i.e., labradorite-bytownite), clinopyroxene, and amphibole, with minor biotite, quartz, and potassium feldspar. We sampled this dioritic part of the pluton at three sites along the Vyhniansky Potok valley between Vyhne and Banky (sites 42, 44 and 45 in Fig. 9(a)), finding it to typically consist of small phenocrysts of plagioclase and augite, no more than ~2-3 mm in size, with biotite also evident near Banky, and to appear unaffected by hydrothermal alteration. These three sites yielded highly variable heat production, ranging from ~4.4 $\mu W\ m^{-3}$ near Banky (site 45 in Table 3) to as low as ~2.1 $\mu W\ m^{-3}$ elsewhere.

The more abundant granodiorite, forming the bulk of the pluton, was described by Chernyshev et al. (2013) on the basis of two very similar samples; they reported major element geochemistry including 62-64% SiO_2 and 3.5-3.6% K_2O, with a summary petrographic description consisting of plagioclase in the compositional range 40-51% anorthite (i.e., andesine-labradorite), biotite, amphibole, potassium feldspar, and quartz, along with other minor constituents. We sampled this lithology at fifteen sites; these were concentrated along the Hodrušsky Potok valley around the former silver mining town of Hodruša-Hámre (sites 15 and 31-34 in Fig. 9(a)), along with the granodiorite inlier below the Hodrušské Jazero reservoir at the upstream end of this valley (sites 13 and 14). We also sampled along the roads leading out of this deeply entrenched valley to the villages of Kopanice, to the south (sites 18-21), and Hadová, to the north (sites 47-50). The NW part of the pluton, in the uplands between the Hodrušsky Potok and Vyhniansky Potok valleys, was not sampled; this area is inaccessible to vehicles and distances within it were too great for sampling on foot in the time available. Everywhere sampled the granodiorite was hydrothermally altered to some extent, the degree of alteration at one site near Hadová (site 48) being sufficient that it is mapped as 'argillite' (see above). The rocks contained plagioclase, hornblende and biotite phenocrysts of typical size ~5 mm, although larger ones, up to ~8 mm, were sometimes present, the plagioclase being typically kaolinized as a result of the hydrothermal alteration. Radioactive heat production ranged from ~2.2 $\mu W\ m^{-3}$ to ~4.9 $\mu W\ m^{-3}$. Composition varied significantly between sites (see, also, below), the largest concentrations of each of the three heat-producing radionuclides being observed in different localities. A sample containing these largest measured concentrations (9.3 wt% K; 11.3 ppm U; and 29.5 ppm Th) would indeed have had heat production of ~5.8 $\mu W\ m^{-3}$, significantly higher than any of our measurements.

Both the granodioritic and dioritic parts of the pluton have heat production far greater than might be predicted from the lithology using the Rybach and Buntebarth (1984) prediction equation, which gives typical values of ~1.8 $\mu W\ m^{-3}$ for granodiorite and ~0.6 $\mu W\ m^{-3}$ for diorite. This demonstrates the need

wherever practicable to base analysis of thermal state on direct rather than proxy measurements. This is already known for other regions such as Britain, where compositionally-similar granitic intrusions have a wide range of heat production (e.g., Lee et al., 1987; McCay, 2016). As will become clear below (section 5.3), the high heat production in the Štiavnica pluton, recognized in the present study, plays a major role in determining the thermal state of the region.

4.5 Andesitic sills and lava flows

Finally, we report 33 sets of measurements of radioactive heat production in the andesitic sills and lava flows surrounding the Štiavnica pluton. Table 3 lists these geographically, grouped by sites ordered clockwise about the pluton starting to the west. The geological mapping shows immense detail regarding these rocks, including a proliferation of subdivisions of classification. It is not clear to us how these differences were established, since forest vegetation obscures the outcrop in most of the region and vegetation-free outcrops were typically only found in new road cuts, which post-date the mapping. It is possible that some of the detail originates from old mine records; however, establishing this would require detailed scrutiny of the local literature, beyond the scope of the present study. The outcrop boundaries depicted on the geological map were, indeed, usually not observable in the field, making it impossible to distinguish sills from lava flows on this basis. Furthermore, as already noted, some of the groupings and classifications, as well as the age order of some of the rocks, differ between the geological map and the Chernyshev et al. (2013) interpretation scheme. Nonetheless, the rocks classified as lavas were either aphyric or contained occasional small plagioclase phenocrysts of ~1-2 mm size, whereas those classified as sills (or small 'stocks' or dykes according to Chernyshev et al., 2013) typically contained plagioclase, augite and hornblende phenocrysts of up to ~5 mm size, the larger phenocrysts being consistent with the slower cooling expected for a sill or small 'stock'. These plagioclase phenocrysts were also typically kaolinized as a result of hydrothermal alteration. Like for other lithologies, Chernyshev et al. (2013) provided a selection of major element analyses and summary petrographic descriptions.

Overall, the measurements indicate a variation of heat production with the phase of the magmatic sequence when the rocks were emplaced, notwithstanding significant variability within each grouping. Thus, for the activity interpreted on the geological map as Middle Badenian (classification codes ending in B2 in Table 3; sites 51 and 52), phase 1 of the magmatism according to Chernyshev et al. (2013), heat production was found to be low, in the range ~1.1-1.4 $\mu W\ m^{-3}$, although this is based on only two sets of measurements (both from the Pukanec area in the south of the region). For the activity interpreted on the geological map as Late Badenian (codes ending in B3) or Middle-Late Badenian (codes ending in B23), some corresponding to phase 1 of the magmatism and some to phase 3 according to Chernyshev et al. (2013), heat production was found to be higher, in the range 1.6-2.0 $\mu W\ m^{-3}$, with one 'hot' outlier at ~2.5 $\mu W\ m^{-3}$. For the phase of sill intrusion interpreted on the geological map as Badenian-Sarmatian (codes ending in BS), corresponding to magmatic phase 2 of Chernyshev et al. (2013) (mostly equating to their 'Banisko Intrusive Complex'), heat production was found to be more variable, but typically even higher, in the range 1.9-2.7 $\mu W\ m^{-3}$, albeit with several 'cold' outliers circa 1.4-1.7 $\mu W\ m^{-3}$ and one 'hot' outlier at ~3.3 $\mu W\ m^{-3}$. Chernyshev et al. (2013) reported a summary petrological description (but no associated geochemical analysis) for a single rock sample from their 'Banisko Intrusive Complex'; this was reported as containing phenocrysts of plagioclase, amphibole, biotite and rare quartz, and was classified as 'quartz-diorite porphyry'. The range of heat production values for this activity overlaps with, but is typically somewhat less than, that for the compositionally similar dioritic part of the Štiavnica pluton, discussed above. It is of course a matter of semantics that rocks consisting of 52-63% normative SiO_2 and with the observed high ratios of plagioclase to potassium feldspar are classified as 'andesite' if part of a lava flow or sill or as 'diorite' if part of a pluton (cf. Streckeisen, 1974).

Some of the sites where we measured heat production in the Sklené Teplice area lie within the Zlatno Intrusive Complex of Chernyshev et al. (2013) (Table 3; sites 58 and 59). These authors regarded this complex as having slightly post-dated the main Štiavnica pluton and having played a unique role in the region's metalliferous mineralization. However, our measured heat production values do not differ from the range observed for the more widespread rocks that they assigned to the 'Banisko Intrusive Complex'. Our samples from localities near Pukanec, which Chernyshev et al. (2013) assigned to their Tatiar Intrusive Complex, likewise yielded unremarkable heat production values (Table 3; sites 53 and 54). Chernyshev et al. (2013) did not present any petrological descriptions or geochemical analyses of rocks that they assigned to the Zlatno or Tatiar intrusive complexes. Although we have not carried out any quantitative modal analysis, either, none of the rocks that we sampled from these localities (or, indeed, from the more widespread Banisko Intrusive Complex), appeared to consist of quartz diorite or granodiorite (requiring 5-20%, or 20-60%, modal quartz, respectively; cf. Streckeisen, 1974). We are, thus, unable to resolve the difference between the classifications of these rocks on the geological map and those reported by Chernyshev et al. (2013); it is unfortunate that they did not indicate field localities where they observed granodiorite within these defined units. We nonetheless note that at one locality, near Kopanice (site 21 in Table 3), rock that was clearly of granodiorite composition in hand specimen fell within an area of outcrop that placed it within the Banisko Intrusive Complex rather than the Štiavnica pluton. Our assessment of this (Table 3) is that the boundary between these rocks had been drawn in the wrong place on the geological map. A possible alternative is that this is indeed a granodioritic part of the Banisko Intrusive Complex, although Chernyshev et al. (2013) did not report that any part of this particular complex is in fact granodioritic. The essential issue, relevant to our present analysis, is that none of the rocks that we investigated, which have been assigned by Chernyshev et al. (2013) to their Zlatno or Tatiar intrusive complexes, had heat production anything like as high as typifies the granodiorite of the main Štiavnica pluton (Table 3).

5…Discussion

We set out to assess the potential value of using a modern portable gamma-ray spectrometer to characterize radioactive heat production in this unfamiliar study region where, as far as we are aware, this technology had not been used before. In a week of fieldwork we collected 62 sets of heat production measurements (Table 3) along with rock samples from most sites to facilitate classification, plus other data that will be published separately. As well as battling with the niceties of the Křovák co-ordinate system and its requirement for maps to be oriented with NNE at the top, and puzzling over the basis whereby, in the absence of exposure, many of the outcrop boundaries shown on the online geological map might have been drawn, various other difficulties were encountered. This online geological map proved to be a most useful resource, although we were surprised at the extent to which its classifications and chronology differ from the more recent work by Chernyshev et al. (2013). This latter publication noted that no proper arguments had been put forward to justify some previous interpretations, but itself provided no arguments to justify some of the proposed revisions. We were also puzzled by some usages of terminology, 'argillite' having already been noted. As another example, was it reasonable for Chernyshev et al. (2013) to classify rock as 'quartz diorite' on the basis of 'rare' quartz phenocrysts, when the specification (Streckeisen, 1974) requires this mineral to exceed 5% of the total of minerals used in classification? One would expect to see a proper modal analysis, or at least a citation of one. Furthermore, although the geological map proved to be accurate in most places, at a few sites it showed incorrect outcrop (see Table 3 for details). Furthermore, in some localities, details provided for location purposes were marked in the wrong places, in some cases as much as ~300 m away from their true locations (as determined by a handheld GPS receiver, in some cases with confirmation using Google Earth); considering that the mapping was reportedly at a scale of 1:10,000, this means that such details were plotted up to ~3 cm away from their 'correct' locations. We have nonetheless established that the granodioritic rocks

of the Štiavnica pluton have significant radioactive heat production, locally approaching 5 $\mu W\ m^{-3}$, making them a significant radiothermal resource. The potential value of a modern portable gamma-ray spectrometer in field reconnaissance of this type is thereby demonstrated.

The rest of this discussion will concentrate on three interrelated key topics: comparison between our estimates of rock composition, using gamma-ray spectrometry, and conventional geochemical determinations; the zoned composition of the Štiavnica pluton; and the vertical extent of this pluton (and its isostatic emplacement mechanism) and its implications for the geothermal resource in the study region.

5.1 Comparisons of estimates of composition

It is evident that some of our raw field measurements (listed in the online supplement) are tightly grouped, whereas others show considerable scatter. This is no doubt in part due to some of the rock surfaces on which the gamma spectrometer was set up not being perfectly flat; as McCay et al. (2014) pointed out, if the rock surrounding a measurement point spans more than a halfspace it will result in a reading that is too high, with readings that are too low resulting if the rock occupies less than a halfspace. However, the fact that the reported radionuclide concentrations do not vary in proportion between the three sets of measurements at each site (see the online supplement for details) indicates that this effect is not the main factor. We are not aware of any previous work on radioactive heat production in this study region, with which our results might be compared. Nonetheless, the scatter in our results can be compared with the manufacturer's specification. Our measurements can also be tested for consistency between adjacent sites in the same lithologies. In addition, our measurements of potassium content can be compared with the geochemical determinations reported by Chernyshev et al. (2013) and with the values from gamma-ray spectrometry reported by Lexa et al. (1999). Finally, one can compare the contributions of the three radionuclides to the heat production at each of the sites.

As already noted, the manufacturer's documentation reports accuracies of ±0.14 wt% for K, ±0.8 ppm for U, and ±1.5 ppm for Th, for measurement runs of three minutes duration. These figures can be compared with the uncertainties (expressed as $\pm 1\sigma$), in the site mean values of compositions, reported in the online supplement. It is thus evident that roughly half of the uncertainties in these site mean values (36 for K, 28 for U, and 27 for Th, each out of 62) fall outside these stated margins. Moreover, at only 13 sites (sites 8, 15, 23, 26, 28, 39, 47, 51, 52, 56, 57, 61 and 62) were the standard deviations for all three radionuclides within the manufacturer's stated tolerances. Although these include some sites with clear planar rock surfaces much larger than the ~1 m^2 area considered *a priori* necessary for the technique to work (sites 15, 28, 61, respectively a vertical rock face adjoining the sealed entrance to a disused mine, a recently excavated road cutting, and a disused quarry) they also include others (notably, sites 8, 23, 26, 39, 47, 51, 52, 56, and 57) where the extent of exposure was borderline for measurement to be attempted.

During the data processing for this comparison, it was realised that many of these larger-than-expected error margins arose because for one of the radionuclides one of the three contributing measurements forms an obvious 'outlier' relative to the other two. Removing these outlying values from the analysis resulted in the set of 'best estimate' radionuclide concentrations and heat production values listed in the online supplement. Processed thus, far fewer concentrations have standard deviations outside the manufacturer's specifications (22 for K, 8 for U, 6 for Th; of those for K, 7 are 0.15 or 0.16 wt%, so only marginally exceed these tolerances), the number of sites with standard deviations for all three radionuclides within these specifications rising to 28 (sites 4, 7, 8, 11, 15, 17, 21, 23, 26, 28, 29, 30, 33, 36, 39, 43, 44, 45, 47, 49, 51, 52, 53, 55, 56, 57, 61, and 62; see the online supplement). However, even so, there remain many sites for which the uncertainties in concentrations still exceed the manufacturer's

stated tolerances. Inspection of the online supplement (where these instances, with standard deviations of at least 10% of the calculated values, are highlighted) indicates that these instances arise for sites where the three measured values for the concentration of a radionuclide are roughly evenly spaced, so one has no basis for discarding any particular value as an outlier. The implication is that if this eventuality arises then one should make at least one additional set of measurements, notwithstanding the increased fieldwork time that will result.

On several occasions we made multiple sets of measurements at adjacent sites in the same lithologies, with the aim of testing the consistency of these measurements. These groupings comprise sites 1, 2 and 3, 7 and 8, 11 and 12, 33 and 34, and 53 and 54 (Table 3; see the online supplement for more details). Other pairs of sites were also documented in adjacent localities, but because they straddle lithological boundaries they are omitted from this comparison. On the basis of the set of analyses for 'mean' heat production, sites 7 and 8, 11 and 12, and 53 and 54 are concordant at the $\pm 1\sigma$ level, whereas sites 1, 2 and 3 and sites 33 and 34 are concordant at the $\pm 2\sigma$ level (see the online supplement). The 'best estimate' values for heat production, with outliers excluded as discussed above, for each pair of sites 7 and 8, 11 and 12, and 53 and 54, have adjusted significantly closer together and, even though the error margins are now much tighter, remain concordant at the $\pm 1\sigma$ level. Sites 1, 2 and 3 remain concordant at the $\pm 2\sigma$ level. However, sites 33 and 34 are no longer concordant. Inspection of the online supplement indicates that this issue has arisen because the highest measurements of K and U for site 33 have been removed as outliers, but these removed values are closer to those measured at site 34 than the values that have been retained. Evidently, the approach adopted of removing outliers on a site by site basis has not given a useful result in this instance. In these cases we should have noted the mismatches while in the field and should thus have undertaken more field measurements until sufficient consistency was achieved. This example indeed demonstrates that significant variations in composition can occur across distances of a metre or so (the typical spacing of repeat measurements at each site) within what appears, in the field, as a homogenous lithology.

Comparisons of radionuclide concentrations between these sites are somewhat more problematic, however. At sites 11 and 12 and sites 53 and 54 all three pairs of 'best estimate' values are concordant at the $\pm 1\sigma$ level, as one might expect. However, at sites 1, 2 and 3 the 'best estimate' values for uranium concentration are concordant at the $\pm 1\sigma$ level, albeit with large margins of uncertainty, whereas for sites 7 and 8 and sites 33 and 34 none of the 'best estimate' radionuclide concentrations are concordant. Thus, although sites 7 and 8 yielded virtually the same heat production, site 8 had significantly higher K and Th concentrations but significantly lower U; the rocks in these two adjacent sites evidently have compositions that differ significantly but which fortuitously result in very similar heat production.

As already noted, Lexa et al. (1999) presented summary results of an airborne gamma ray spectrometry survey of the Štiavnica upland. These workers only reported potassium concentration, so the comparison is restricted to this radionuclide. The values they obtained are 2-3 wt% in both the granodioritic and dioritic parts of the Štiavnica pluton, and typically <2 wt% in the other Miocene igneous rocks, thus underestimating this parameter, relative to our own results, by a typical factor of ≥ 2. Lexa et al. (1999) provided no details of the measurement procedure used; we thus cannot account for this discrepancy. We suspect that the underestimation evident from their results might have led to the lack of recognition in the extant literature of the importance of radioactive heat production in this vicinity.

A comparison with the results of Chernyshev et al. (2013), grouping all samples from four key rock units, and scaling the numerical values to express the geochemical determinations as percentages by weight of

K, not K_2O, is presented in Table 4. The two methods give reasonable agreement for the (?) late Middle Pleistocene Brehy basalt (represented by our site 17) and the andesitic lavas of the Studenec Formation, from phase 3 of the Štiavnica magmatism (represented by our sites 4, 16 and 38). Nonetheless, for the dioritic and granodioritic rocks of the Štiavnica pluton, the typical concentrations of K_2O, derived from gamma ray spectrometry measurements, greatly exceed those obtained by geochemical analysis. However, the large margins of uncertainty listed in Table 4 indicate that the compositions of these lithologies vary from place to place, as we had already deduced on other grounds.

Table 4 here: comparisons of potassium content

Taking account of the possibility of lateral variations in composition, a more appropriate test is to compare measurements from sites in close proximity. However, none of our sites in the rocks of phase 1 or phase 3 of the Štiavnica magmatism was anywhere near the co-ordinates reported by Chernyshev et al. (2013) for any of their samples. Furthermore, no comparison is possible for any of the minor dioritic intrusions assigned to phase 2 of this magmatism, because Chernyshev et al. (2013) did not report geochemical analyses for any of these rocks. Direct comparisons for sites in close proximity are, however, possible for the Brehy basalt and for both the dioritic and granodioritic parts of the main Štiavnica pluton. If we had had access to the online supplement of the Chernyshev et al. (2013) paper, containing their site co-ordinates and geochemical analysis results, at the time of our fieldwork, we could, of course, have visited the precise localities where they sampled, although there is no guarantee that flat rock surfaces suitable for gamma-ray spectrometry measurements would have been available.

As noted in Table 4, Chernyshev et al. (2013) analysed three samples of the Putikov Vršok basalt. Two of these were collected near the neck, several kilometres from our site 17 at the distal end of this flow unit, near Brehy, where this basalt cascaded onto the valley floor of the River Hron. Their third sample (S-B3/02; with reported co-ordinates that convert to UTM 34U CU 24886 63881, or Křovák -458295 -1262367), came from a point ~500 m north of our site, likewise at the distal end of the flow unit. Their measurement, 1.93 wt% K_2O or 1.60 wt% K, falls within the margin of uncertainty of ours, 1.78$\pm$0.35 wt% K ($\pm 2\sigma$), our three raw measurements being 1.67, 1.68, and 1.98 wt% K (see the online supplement).

The Chernyshev et al. (2013) sample of diorite from the Štiavnica pluton (St-4/08; with reported co-ordinates that convert to UTM 34U CU 41255 72641, or Křovák -441509 -1254437) came from a point ~300 m WSW of one of our sites (site 44; Table 3). As already noted, our site was in the floor of the Vyhniansky Potok valley, between Vyhne and Banky, whereas theirs was in a tributary valley to the south. Their measurement, 1.52 wt% K_2O or 1.26 wt% K, falls below the lower limit of the margin of uncertainty of ours, 2.26$\pm$0.60 wt% K ($\pm 2\sigma$). Our three measurements, 2.08, 2.61, and 2.10 wt% K, were indeed all significantly higher than the result of their analysis.

Finally, one of the Chernyshev et al. (2013) granodiorite samples from the Štiavnica pluton (St-2/04; with reported co-ordinates that convert to UTM 34U CU 35345 69296, Křovák -447579 -1257482), from the Hodrušské Potok valley at Hodruša-Hámre, came from a point near two of our sites (being ~200 m ESE of site 15 and ~300 m NE of site 31; Table 3). However, their measurement, 3.56 wt% K_2O or 2.96 wt% K, falls well below ours, 5.56$\pm$0.25 and 6.32$\pm$0.53 wt% K ($\pm 2\sigma$). Our two groups of three measurements, 5.70, 5.49, and 5.48 wt% K, and 6.52, 6.02, and 6.42 wt% K, were likewise all much higher than their analysis result.

Taking into account the fact that compositional zoning is to be expected within granodiorite plutons (e.g., Bateman and Nokleberg, 1978; Tindle and Pearce, 1981; see, also, below), especially near their edges,

that our measurements show clear evidence of compositional variability in both the dioritic and granodioritic parts of the Štiavnica pluton, and that our measurements agree well with those of Chernyshev et al. (2013) in the Brehy basalt, in which near homogenous composition can be expected, we attribute the mismatches between our results and theirs regarding the potassium content of the Štiavnica pluton to compositional variation within this pluton. The impression created by the Chernyshev et al. (2013) paper, of uniform composition of both the dioritic and granodioritic parts of the pluton, would therefore appear to be an artefact of the small number of samples that they analysed.

Regarding the effects of the different radionuclides, one expects uranium to be the most significant contributor to heat production (e.g., Birch, 1954; McCay et al., 2014; Attia and Wahid, 2016). However, using the aforementioned 'best estimate' values for composition, at the majority of our sites, 34 out of 62 or ~55%, thorium made the largest contribution to heat production (see the online supplement). Uranium made the largest contribution at 26 sites, or ~42%, with potassium the largest contributor at the remaining 2 sites or ~3%. This latter grouping comprised site 25 near Kopanice and site 51 near Pukanec; both these sites are in localities where minor dioritic intrusions of magmatic phase 2 pervade lavas of phase 1; site 25 being in the older lava with site 51 in a dioritic intrusion (Table 3). Of the remaining samples, the largest percentage contribution to heat production from thorium, ~57% of the total, was observed at another site (site 1) in a phase 2 dioritic intrusion. Thorium also makes the greatest contribution at site 45, near Banky, where particularly high heat production was determined in the dioritic part of the Štiavnica pluton (Table 3). On a 'best estimate' basis the heat production at this site is ~4.5 $\mu W\ m^{-3}$, as a result of ~30 ppm of thorium, the highest concentration measured in the region (see the online supplement). Nonetheless, uranium is the largest contributor at the sites within the Štiavnica granodiorite with heat production >4 $\mu W\ m^{-3}$ (i.e., at sites 14, 49 and 50) and indeed makes the largest percentage contribution (~57%) at the site (site 50) with the greatest heat production, ~4.9 $\mu W\ m^{-3}$ on a 'mean' basis (Table 3) or ~5.0 $\mu W\ m^{-3}$ on a 'best estimate' basis (online supplement), this site having the highest uranium concentration (~11 ppm) measured in the region. These sites with relatively high heat production thus conform to the expected pattern with uranium the most significant contributor to heat production. The measured uranium concentrations are indeed particularly variable, for example within the Štiavnica granodiorite they vary between ~2.0 and ~10.8 ppm for site means (Table 3) and between ~1.1 and ~11.3 ppm for individual measurements (online supplement), and thus make a significant contribution to variations in heat production even for the 'colder' rocks in the region. Furthermore, although one expects uranium content to increase inward from the margins of a granodioritic pluton, reflecting its zoned composition (e.g., Rybach, 1976; see also below), some sites well inside the pluton have low uranium concentrations (Table 3). We infer the cause of this to be the high solubility that uranium can attain under environmental conditions (e.g., Casas et al., 1998; Elless and Lee, 1998; Gorman-Lewis et al., 2008; Attia and Wahid, 2016) combined with the hydrothermally altered state of many samples that (by breaking down the crystal structure of the mineral grains in which the uranium would have been concentrated in the original rock) is likely to facilitate uranium release. On this basis, the measurements with the highest uranium concentrations and heat production values are likely to provide the best estimates for rocks in the Štiavnica pluton that have not been affected by hydrothermal alteration or surface environmental conditions.

With hindsight, an improved field procedure at each site, instead of always making three sets of measurements, would have been to keep making repeat measurements until three sets of values were obtained that were consistent within a certain margin (say, $\pm$10%, or $\pm$ the margins of uncertainty stated in the manufacturer's documentation) for each of the three radionuclides, or for the radionuclide that makes the largest contribution to heat production, then to discard any other measurements as outliers. However, a practical difficulty that would thus arise in the present study region would be the limited

exposure, as already noted; at most sites the small area of visible outcrop would restrict the maximum number of repeat measurements. Although the main aim has been to obtain measurements of heat production, rather than radionuclide concentrations, we do not recommend basing a field protocol on consistency of measured heat production values. This is, first, because of the possibility that sites with rocks of different composition may fortuitously have the same heat production, as is apparent for sites 7 and 8 (see above, also the online supplement). Furthermore, achieving any margin of consistency regarding heat production (or the contribution to heat flow from any particular radionuclide) would have been impossible during this fieldwork as we had no means of determining this quantity in the field (it was calculated in the evenings after days in the field); to introduce such a requirement in future would mean taking a tablet PC or pocket calculator into the field, unless the manufacturer were to modify the software in their instrument to provide the necessary readout. An alternative way of achieving increased accuracy would be to increase the measurement duration; the 'Gamma Surveyor II' can be set up to measure for 5, 10, 20, or 30 minutes, rather than the standard 3 minutes. However, the manufacturer's documentation does not provide any quantitative indication regarding how a given increase in measurement time results in any particular increase in accuracy. Such documentation has been provided for older equipment (e.g., Løvborg, 1984), and can serve as a guide, but is specific to the detector being used.

5.2 Zoned composition of the Štiavnica pluton

Our results, discussed above, indicate significant variability in the composition of the Štiavnica pluton, in contrast with its portrayal (on the geological map and by Chernyshev et al., 2013) as consisting of parts of uniform granodioritic and dioritic composition with an inferred boundary between the Hodrušsky Potok and Vyhniansky Potok valleys. Although many workers (e.g., Nemčok et al., 2000; Chernyshev et al., 2013) have stated that the dioritic part of the pluton is older, reported numerical ages for the two parts are indistinguishable (13.3±0.2 Ma for the diorite and 13.4±0.2 and 13.3±0.6 Ma for the granodiorite, all ±2σ, from Chernyshev et al., 2013). We did not locate the discrete boundary between these lithologies, reported on the available geological mapping (Fig. 7), so are unable to confirm whether there were two separate intrusions or a single intrusion with gradational composition. Nonetheless, many previous studies have identified zoned compositions of granodioritic intrusions, with rocks becoming progressively less mafic away from the margins of the intrusion. For example, Bateman and Nokleberg (1978) studied the Mount Givens granodiorite of the Sierra Nevada Mountains, California. This ~80 km by ~15 km pluton of Cretaceous age varies progressively in composition from tonalite at the rim to granodiorite then granite at the core. These authors explained this effect as a consequence of crystal fractionation within the magma: as the pluton cooled inwards, relatively mafic mineral phases with relatively high freezing points tended to accrete to the margins of the magma chamber. As another example, Tindle and Pearce (1981) studied the Loch Doon granodiorite of SW Scotland. This ~20 km by ~10 km pluton of Caledonian (Devonian) age varies progressively in composition from diorite at the rim to quartz diorite, then tonalite, then granodiorite, with granite at the core. These authors recognized effects of magmas of different composition, but nonetheless regarded crystal fractionation as the principal cause of the observed variability. In both these case studies, the compositional gradient was greatest near the rim of the pluton. Other instances of granodiorite zonation have been explained as a consequence of distinct emplacement phases separated by intervals of ten million years or more (e.g., Miles et al. 2014); however, this possible explanation is inapplicable in the case of the Štiavnica pluton given the limited duration of its intrusive phase (Chernyshev et al., 2013). Counterexamples demonstrating 'inverse' zonation, with radioactive heat production increasing towards the margins of granitic intrusions, have also been noted, for example in the Mont Blanc granite of the Alps (Rybach et al., 1966), and can be explained as a result of migration of residual melt during solidification (Rybach and Buntebarth, 1981).

At each set of sites where we undertook a traverse perpendicular to the margins of the Štiavnica pluton our results indicate (notwithstanding substantial fluctuations) increases in heat production, typically associated with increases in uranium content, towards the pluton interior. Thus, first, near the SW limit of the pluton at the western end of Hodruša-Hámre, one of our sites (31 in Table 3) was located very near (~100 m north of and ~50 m below) the intrusive contact between granodiorite and country rock; it yielded heat production of ~2.2 $\mu W\ m^{-3}$. In this vicinity, the country rock is mapped as Mesozoic sediments (the Early Triassic Benkov Formation or benkovské súvrstvie, comprising sandstone and mudstone, and the Late Triassic Gutenstein Formation or gutensteinské súvrstvie, comprising limestone). A nearby site (15 in Table 3), farther from the pluton margin (~160 m north of it and ~80 m below it) yielded heat production of ~3.3 $\mu W\ m^{-3}$. Second, a similar effect is observed farther east, where measurements along the road between Hodruša-Hámre and Kopanice (sites 18-21), at points ~300-600 m away from and ~50-100 m below the intrusive contact yielded heat production of ~2.5-2.9 $\mu W\ m^{-3}$. Farther away from this intrusive contact (~700 m from it and ~200 m below it), north of the eastern end of Hodruša-Hámre, another site (34 in Table 3) yielded heat production of just under 4.0 $\mu W\ m^{-3}$. Third, along the traverse west of Hadová the heat production ranges from ~3.5 $\mu W\ m^{-3}$ at the eastern edge of the granite outcrop (site 47) to ~4.9 $\mu W\ m^{-3}$ ~350 m farther west (site 50), this being the highest heat production value that we observed. These sites are ~200-450 m away from, and probably ~100-200 m below, the contact with rocks of magmatic phase 1 to the southeast. However, immediately east of these sites at the eastern edge of the granite outcrop (separated by a zone of 'argillite', so contact relations are unclear) is an outcrop of dioritic rocks of the 'Banisko Intrusive Complex' of Chernyshev et al. (2013). These persist eastward for several kilometres, although likewise only hundreds of metres from the contact (to the south) with older rocks, and have heat production in the range ~1.9-2.7 $\mu W\ m^{-3}$ (including sites 6, 7, 8 and 46 in Table 3). In the light of the previous observations of compositional zoning in other plutons, we tentatively suggest that these rocks might represent the relatively mafic rim of the Štiavnica pluton, rather than being a separate set of small stocks, of almost the same age as this pluton and clustered around it, as Chernyshev et al. (2013) have suggested. By analogy, the contact between granodiorite forming a small outlier of the Štiavnica pluton near the Hodrušské Jazero reservoir (sites 13 and 14, with heat production ~3.1-4.1 $\mu W\ m^{-3}$) and rocks of the 'Banisko Intrusive Complex' ~300 m farther southeast (sites 10-12, with heat production ~2.3-3.3 $\mu W\ m^{-3}$) might provide further evidence of compositional zonation near the rim of what is in reality a single pluton. It follows that another compositional gradient might exist, southward between the dioritic northern part of the Štiavnica pluton (around Vyhne and Banky) and its granodioritic more central part (around Hadová), rather than the abrupt boundary between these two parts depicted on the geological map (Fig. 7) and by Chernyshev et al. (2013). The most obvious departure from the characteristic inward trend of increasing heat production is the observation (at site 45, near Banky) of one of the highest measurements (~4.4 $\mu W\ m^{-3}$) at a point within metres of the mapped intrusive contact (adjoining metamorphic basement; schist and slate) at the northern rim of the pluton. At this stage we can offer no explanation for this apparently contradictory observation, other than to repeat that the composition of the diorite was different at this site from that which we sampled elsewhere; it is apparent from this anomaly and much else that this study region will benefit from more detailed investigation, beyond the scope of the present study. Pending further investigations, the Hadová traverse arguably provides the clearest evidence of compositional zonation of the Štiavnica granodiorite; in addition to the aforementioned increase in heat production away from the margin of the pluton, corresponding increases in potassium and uranium concentration and in the proportion of the heat production caused by the uranium are also here evident (see Table 3 and the online supplement).

5.3 Thermal state of the study region

In principle, one might hypothesize given the young age of the Štiavnica pluton (~13 Ma; Fig. 3) that it might still be cooling following intrusion and the resulting transient heat loss might explain the higher heat flow relative to surrounding areas (Fig. 4). Nemčok et al. (2000) presented calculations for cooling at the 2.5 km depth of the top of a cylindrical pluton of 10 km diameter and 7 km vertical extent, at which depth the temperature prior to intrusion was assumed to have been 100 °C. The temperature at the centre of the top of the pluton was calculated to have been 750 °C on intrusion, decreasing to ~440 °C after one million years and ~350 °C after two million years, at which points in time the calculated cooling rate was ~150 °C Ma^{-1} and ~50 °C Ma^{-1}. These authors envisaged that this cooling occurred in part by thermal conduction and in part as a result of erosion, but did not fully specify their solution so it is not reproducible. Nonetheless, the progressively-decreasing cooling rates over time expected, in general (cf. Carslaw and Jaeger, 1959), for solutions of this type imply (given the ~13 Ma timing of emplacement; see above) that significant residual heat remains present, potentially explaining the local high heat flow anomaly (Fig. 4).

However, the above scenario, of slow cooling of the pluton and its surroundings by heat conduction alone, leaving significant residual heat in the subsurface to the present day, is at odds with the rapid cooling indicated by the brief duration of the hydrothermal mineralization, for example the evidence of temperature well below 300 °C within two million years intrusion (section 2). A likely reason for this mismatch is that the published calculations underestimate the rate of heat loss from the pluton by omitting any effect of hydrothermal circulation in its surroundings; Nemčok et al. (2000) stated that the inclusion of hydrothermal circulation would over-complicate their model.

We are not aware of any published solution for cooling of a solid cylinder by convection in its surroundings. However, solutions exist for a sphere (e.g., Luikov, 1968), and have been implemented as online calculators (e.g., by Recktenwald, 2013, using Matlab and by Binous and Higgins, 2013, using Wolfram Mathematica). Since the Štiavnica pluton is roughly equidimensional, these solutions can be applied to it as an approximation. Cooling of a sphere of radius R, thermal conductivity k and thermal diffusivity κ by fluid circulation in its surroundings depends on its Biot number, Bi, defined as $h \times R/k$, where h is the heat transfer coefficient relative to the surroundings. Fluid circulation outside the pluton is expected to cause $h >> k/R$, so $Bi >> 1$; in these circumstances the timescale τ required for the sphere to cool to its final steady-state temperature will approximate R^2/κ. Taking κ ~1 mm^2 s^{-1} as a rough estimate for granitic rocks, one obtains for example τ ~0.8 million years for R=5 km or ~1.8 million years for R=7.5 km. The larger of these values, consistent with a pluton of diameter ~15 km (cf. Figs 3, 6(a)), can thus roughly account for the reported duration of the hydrothermal activity. It follows that the transient cooling following the intrusion of this pluton ended circa the beginning of the Late Miocene; the small size of the pluton means that it is much too old to maintain a transient thermal anomaly. Since the ~40 mW m^{-2} excess heat flow in the Štiavnica upland relative to its surroundings (Fig. 4 and Tables 1 and 2) is evidently not a transient effect of cooling of the Štiavnica pluton, alternative potential explanations will now be considered.

Figure 10 here: model geotherms

An initial potential explanation of this heat flow anomaly is to assume that the measured heat production as high as ~5 μW m^{-3} is representative throughout the vertical extent of the Štiavnica pluton. To account for the observed heat flow anomaly on this basis, under steady-state conditions, the pluton would therefore need to be ~40 mW m^{-2} / ~5 μW m^{-3} or ~8 km thick. Solution 1 in Fig. 10 is calculated on this basis. As an alternative, it can be assumed that the heat production is concentrated in the upper part of the pluton, possibly as a result of upward migration of residual melt during solidification (cf. Rybach and

Buntebarth, 1981). Solution 2 in Fig. 10 is calculated on this basis, assuming downward exponential decay in heat production over a characteristic scale depth of 8 km. Either of these solutions can account for a near-surface geothermal gradient of ~36.7 °C km^{-1}, consistent with the observed ~110 mW m^{-2} surface heat flow for a thermal conductivity of 3 W m^{-1} °C^{-1}. Solution 3 shows an alternative solution for the geotherm, consistent with the same surface heat flow, in which the upward increase in geothermal gradient is caused by erosion (again, under steady-state conditions) with no contribution from radioactive heat production; the required erosion rate is rather high, 1.39 mm a^{-1}. This is evidently an end member of a range of possibilities; solutions 4 and 5 illustrate the combined effects of erosion and radioactive heat production, both of which can again account for the measured surface heat flow. Solution 4 assumes a scale depth for the radioactive heat production of 4 km and an erosion rate of 0.96 mm a^{-1}, whereas solution 5 assumes a scale depth of 8 km and an erosion rate of 0.28 mm a^{-1}. Overall, these solutions demonstrate a point noted by Westaway (2002), that radioactive heat production and erosion rates can trade off against each other to produce very similar geotherms. Other solutions for the geotherm might also be feasible, taking account of the non-steady-state conditions that might be expected as a result of changing erosion rates caused by climate change during the Pleistocene (cf. Bridgland and Westaway, 2008a; Westaway et al., 2009), but are beyond the scope of the present study.

As already noted, the uplift rate indicated by the Hron terrace staircase has been ~0.15 mm a^{-1} since the early Middle Pleistocene, which would require a spatial average erosion rate of, likewise, ~0.15 mm a^{-1}, if the landscape is in a steady state. The greater relief of the Štiavnica upland, compared with the Hron valley, implies higher rates of uplift and denudation (cf. Westaway, 2002). Conversely, if the Štiavnica pluton was unroofed at a steady rate, this rate can be estimated as ~2500 m / 13 Ma or ~0.2 mm a^{-1}; climate change during the Pleistocene might be expected to have caused this rate to be exceeded. Overall, we consider that the thermal state of the Štiavnica upland might be governed by an erosion rate as high as several tenths of a millimetre per year. This implies, given the range of solutions for the thermal state in Fig. 10, that the radioactive heat production in the pluton is maintained over a substantial vertical extent (scale depth or extent of uniform heat production approaching 8 km).

5.4 Isostatic equilibrium of the study region

One might also address the Štiavnica upland through considerations of isostasy, utilizing the measured Bouguer gravity anomalies (Figs 5 and 6(c)). It is well established that the radioactive heat production in crystalline rocks shows a general inverse correlation with density (e.g., Rybach and Buntebarth, 1982, 1984), as a result of lower density having a general correlation with content within the crystal structure of relatively large cations such as potassium. Clearly, if the isostatic configuration of the Štiavnica upland were simply due to the presence of relatively low-density granitic rocks surrounded by higher-density country rock, as is widely observed elsewhere (e.g., Bott and Masson-Smith, 1957), one would be readily able to make estimates of the mass deficit associated with the intrusion from the magnitude of its gravity anomaly and by applying standard theory (derivable subject to the standard assumption of Airy isostasy) linking the uplift over it to its density contrast and vertical extent. The top of the pluton near its centre is ~800 m above sea-level, where in many localities it is overlain by maybe ~100 m of country rock, comprising the various sedimentary and metamorphic formations already mentioned. Remšík et al. (2001) have reported that the top of 'pre-Tertiary' basement in the caldera, on the NE, eastern and SE flanks of this pluton, is ~1500 m below sea-level. The average height of the present-day land surface in these localities within the caldera is ~500 m, but the evidence from the Kalvária and Kyhisýbel necks, which erupted through the caldera fill (Fig. 3), indicates, say, ~500 m of local erosion. Neglecting any thickness of rocks other than those emplaced during the phase of caldera filling (phase 3 in Fig. 3), the full thickness of caldera fill, preceding erosion, can thus be estimated as ~2500 m. One may therefore estimate, very crudely, that during the development of the 'resurgent horst' the top of the Štiavnica pluton has uplifted

by ~2300 m (from ~1500 m below to ~800 m above sea-level) in response to the erosion of the presumed same former thickness of ~2500 m of caldera fill (cf. Nemčok et al., 2000) that formerly overlay it. The rough equivalence between these instances of uplift and denudation is as expected for isostatic compensation of erosion under steady-state conditions (e.g., Westaway, 2002).

Nonetheless, as already discussed, the densities of the granodiorite and the basement rocks though which it intruded are similar; this particular case study thus does not follow the usual pattern of granitic intrusions having significantly lower density than the surrounding country rock. We investigate this issue using the Bouguer gravity anomaly dataset (Figs 5 and 6(c)). In the Javorie upland, the Bouguer anomaly is -19 mgal at Vigľašská Huta - Kalinka (at the point marked in Fig. 5) it rises to a maximum of -17 mgal ~5 km farther east, and decreases to -28 mgal ~2 km farther north and ~3 km farther west and to -22 mgal ~2 km farther south. There is indeed no simple pattern of a negative Bouguer gravity anomaly associated with a low-density granitic pluton, as might have been expected.

In the Štiavnica upland, the Bouguer gravity anomaly is -22 mgal at Banská Štiavnica (at the point marked in Fig. 5; see, also, Fig. 6(c)). It decreases westward to a minimum of -23 mgal at the centre of the Štiavnica pluton, with higher values, circa -21 m at the northern and southern margins of the pluton around Vyhne and Hodruša-Hámre. In the 'resurgent horst' it rises to -16 mgal in the south around Vysoká, but decreases to a minimum of -24 mgal (i.e., less than at the centre of the pluton) in the north around Sklené Teplice. In the caldera, the Bouguer anomaly reaches minima of -26 mgal southeast, -30 mgal east, and -39 mgal northeast of Banská Štiavnica. The pluton thus has a very small negative Bouguer anomaly compared with the -20 mgal mean of the values in the rest of the resurgent horst, but it has a positive Bouguer anomaly relative to the circa -32 mgal mean for the surrounding caldera. Here, too, there is thus not the 'expected' pattern of a negative Bouguer anomaly relative to higher-density surroundings; the caldera fill is evidently less dense than the pluton itself.

Chernyshev et al. (2013) alluded to one potential explanation for the uplift of the Štiavnica 'resurgent horst', first suggested by Konečny (1971), as a consequence of intrusion of rhyolitic magma synchronous with the rhyolitic eruptions during phase 5 of the magmatism (Fig. 3). This concept appears to have arisen because Konečny (1971) envisaged an analogy with the Valles caldera in the western USA (cf. Smith et al., 1961), which experienced large-scale rhyolitic activity in the Early Pleistocene. We do not see any clear analogy between these two magmatic centres; nonetheless, this hypothesis can be tested using the gravity dataset, by calculating the difference in Bouguer gravity anomaly Δg as a result of the presence of a laterally infinite layer of thickness H and density contrast $\Delta\rho$, using the standard slab formula:

$$\Delta g = 2 \pi \Delta\rho G H , \qquad (2)$$

where G is the universal gravitational constant. From Tenzer et al. (2011), rhyolite has a typical density of 2207 ± 225 kg m^{-3} ($\pm 1\sigma$), making $\Delta\rho$ circa -500 kg m^{-3} relative to the local basement rocks. Thus, if the ~2500 m of uplift of the 'resurgent horst' was a consequence of intrusion of H=2500 m thickness of rhyolite (cf. Konečny, 1971), a resulting Bouguer anomaly of circa -50 mgal can be predicted. However, no such anomaly is evident between this horst and its surroundings (Fig. 6(c)); indeed, as has been noted above and in this Figure, the Bouguer anomaly is more positive in the resurgent horst. Notwithstanding its standing within the local literature, this particular hypothesis can now be excluded. On the contrary, the principal density contrast influencing the present-day configuration is between the H=2000 m maximum thickness of andesitic fill in the caldera (typical density ~2470 kg m^{-3}; see above) and the pluton and basement in the 'resurgent horst' (typical density ~2700 kg m^{-3}; see above). Using the resulting value of $\Delta\rho$=-230 kg m^{-3}, equation (2) gives Δg=-19 mgal, consistent with the observed maximum variation

(between -39 mgal in the caldera and -20 mgal in the resurgent horst; see above). The local variation in Bouguer anomalies is thus consistent with this choice of densities, including the assumption that the granodiorite is indeed no less dense than the basement rocks into which it intruded.

This lack of a negative Bouguer anomaly relative to its surroundings raises the obvious question as to how the Štiavnica pluton was able to ascend in the first place. We suggest that this was feasible, because at its time of solidification and emplacement this mass of granitic rock was hotter than at present, so as a result of thermal expansion its density was lower. Many studies have established that minerals present in the pluton, such as hornblende and ~50% calcic / ~50% sodic plagioclase, freeze at ~800 °C, providing a rough indication of the solidification temperature of this pluton. The density change $\Delta\rho$ in any isotropic material, as a result of thermal expansion accompanying a temperature rise ΔT, can be expressed as

$$\Delta\rho = -3\,\alpha\,\rho_o\,\Delta T\,, \qquad (3)$$

where ρ_o is the initial density and α the coefficient of linear expansion. The value of α for granitic rocks can be taken (e.g., from http://www.engineeringtoolbox.com/linear-expansion-coefficients-d_95.html) as 7.9×10^{-6} °C^{-1}. Taking ρ_o=2700 kg m^{-3}, as before, one thus obtains $\Delta\rho$=-51 kg m^{-3} for ΔT=800 °C.

As regards the conditions that may be inferred during ascent of the granodiorite, with $\Delta\rho$=-51 kg m^{-3} (the inferred typical difference between granodiorite at its freezing point and basement under ambient conditions) and H=8000 m one obtains (using equation (2)) Δg=-17 mgal. This exceeds the typical difference between the present-day Bouguer gravity anomalies in the pluton (estimated as -22 mgal) and in the surrounding caldera (estimated as -32 mgal), suggesting that at its time of emplacement the density of the pluton was low enough to enable it to rise relative to the caldera, even though its density now, after it has cooled, is too high. Although this argument does not help to constrain the thickness of the pluton directly, and notwithstanding the approximations involved, it requires the pluton to have a substantial thickness; for example if it were only 3000 m thick then cooling would have only increased its Bouguer gravity anomaly by ~6 mgal, indicating that at its time of emplacement it would have been too dense to rise. Furthermore, it is evident that once the pluton had cooled to present conditions, the continued uplift across it (revealed by the local geomorphology) could no longer have been sustained by its buoyancy, and is evidently instead being driven as an isostatic consequence of continuing erosion (as was inferred in section 5.3). The heat production within this pluton (Table 3) warrants recognition as a significant factor contributing to the geothermics of the region, previous works (e.g., Remšík et al., 2000, 2001) having regarded this region's thermal groundwater as heated through circulation at depth, without consideration of local radioactive heat production.

6…Conclusions

We have reported 62 sets of measurements of radioactive heat production from central-southern Slovakia, obtained using a modern portable gamma-ray spectrometer. The majority of these determinations are for intrusive and extrusive igneous rocks of the Late Cenozoic Central Slovakian Volcanic Zone; however, we have also made some determinations, for comparison, from (pre-) Variscan basement rocks. Sites in granodiorite of the Štiavnica pluton are thus shown to have heat production in the range ~2.2-4.9 μW m^{-3}, this variability primarily reflecting variations in content of the trace element uranium. Sites in dioritic parts of this pluton have a lower, but overlapping, range of heat production, ~2.1-4.4 μW m^{-3}. Sites that have been interpreted in adjoining minor dioritic intrusions of similar age have heat production in the range ~1.4-3.3 μW m^{-3}. The composition of the main Štiavnica pluton is zoned, with potassium and uranium content and radioactive heat production typically increasing inward from its

margins, reflecting variations observed in other granodioritic plutons elsewhere (e.g., Bateman and Nokleberg, 1978; Tindle and Pearce, 1981). It is indeed possible that the adjoining dioritic rocks, hitherto assigned to other minor intrusions of similar age, located around the periphery of the Štiavnica pluton, in reality provide further evidence for zonation of the same pluton. The vicinity of this pluton is associated with heat flow ~40 mW m^{-2} above the regional background. On the basis of our heat production measurements, we thus infer that the pluton has a substantial vertical extent, our preferred estimate for the scale depth for downward decrease in radioactive heat production being ~8 km. Nonetheless, this pluton lacks any significant negative Bouguer gravity anomaly. We attribute this to the effect of the surrounding volcanic caldera, filled with relatively low-density lavas, 'masking' the pluton's own gravity anomaly. We envisage that emplacement of this pluton occurred when it was much hotter, and thus of lower density, than at present, its continued uplift, evident from the local geomorphology, being the isostatic consequence of localized erosion. The heat production in this intrusion evidently plays a significant role, hitherto unrecognized, in the regional geothermics.

Online supplement

Acknowledgements
We are most grateful to the manager of a geothermal energy company, interested in developing resources in the study region, who does not wish to be publically identified for commercial reasons. We thank him for organizing an initial introductory visit to the region and for arranging for many helpful discussions with Slovakian researchers, which facilitated our understanding of the region. Daniel Marcin kindly provided an electronic copy of the Franko et al. (1995) monograph. We thank Ladislaus Rybach and two anonymous reviewers for their thoughtful and constructive comments.

References

Alasonati-Tašárová, A., Afonso, J.C., Bielik, M., Götze, H.-J., Hók, J., 2009. The lithospheric structure of the Western Carpathian–Pannonian Basin region based on the CELEBRATION 2000 seismic experiment and gravity modelling. Tectonophysics, 475, 454–469.

Attia, T.E., Wahid, A.M., 2016. Role of uranium in controlling radiogenic heat production based on gamma ray spectrometry and thermal remote sensing data, southwestern Sinai, Egypt. Environmental Earth Sciences, 75 (296), 17 pp; doi: 10.1007/s12665-015-5131-y

Bajtoš, P., 2001. Low enthalpy geothermal energy from mine waters in Slovakia. Proceedings of International Scientific Conference "Geothermal Energy in Underground Mines", Ustroñ, Poland, 21-23 November 2001, 4 pp. Available online: http://kgp.wnoz.us.edu.pl/Pdf/a11.pdf (accessed 22 July 2016)

Bahna, B., Chovan, M., 2001. Low-sulfidation type of epithermal Au-Ag mineralization near Pukanec (Central Slovakia Neogene volcanic fields). GeoLines, 13, 11-17.

Bateman, P.C., Nokleberg, W.J., 1978. Solidification of the Mount Givens granodiorite, Sierra Nevada, California. Journal of Geology, 86, 563-579.

Bielik, M., Alasonati-Tašárová, Z., Zeyen, H., Dérerová, J., Afonso, J.C., Csicsay, K., 2010. Improved geophysical image of the Carpathian-Pannonian Basin region. Acta Geodaetica et Geophysica Hungarica, 45, 284–298.

Bauer, V., 1999. Mining of gold and silver deposit in Slovak Republic. Publications of the University of Miskolc, Series A. Mining, 53, 277-288.

Bella, P., Gaál, Ľ., Grego, J., 2010. Hydrothermal quartzite caves in the Šobov quarry near Banská Štiavnica, Slovakia. Acta Carsologica Slovaca, 48 (1), 19–30.

Bella, P., Gaál, Ľ., Šucha, V., Koděra, P., Milovský, R., 2016. Hydrothermal speleogenesis in carbonates and metasomatic silicites induced by subvolcanic intrusions: a case study from the Štiavnické vrchy Mountains, Slovakia. International Journal of Speleology, 45 (1), 11-25.

Bielik, M., 1999. Geophysical features of the Slovak Western Carpathians: a review. Geological Quarterly, 43, 251-262.

Bielik, M., Majcin, D., Fusán, O., Burda, M., Vyskočil, V., Trešl, J., 1991. Density and geothermal modelling of the Western Carpathian Earth's crust. Geologica Carpathica, 42, 315-322.

Bielik, M., Šefara, J., Kováč, M., Bezák, V., Plašienka, D., 2004. The Western Carpathians—interaction of Hercynian and Alpine processes. Tectonophysics, 393, 63-86.

Binnie, S.A., Phillips, W.M., Summerfield, M.A., Fifield, L.K., 2007. Tectonic uplift, threshold hillslopes, and denudation rates in a developing mountain range. Geology, 35, 743-746.

Binous, H., Higgins, B.G., 2013. Transient cooling of a sphere. Available online: http://demonstrations.wolfram.com/TransientCoolingOfASphere/ (accessed 29 December 2016)

Birch, F., 1954. Heat from radioactivity. In: Faul, H., Nuclear Geology. Wiley, New York, pp. 148–174.

Boldizsár, T., 1964. Terrestrial Heat Flow in the Carpathians. Journal of Geophysical Research, 69, 5269-5275.

Bott, M.H.P., Masson-Smith, D., 1957. The geological interpretation of a gravity survey of the Alston Block and the Durham Coalfield. Quarterly Journal of the Geological Society, London, 113, 93-118.

Bridgland, D.R., 2000. River terrace systems in north-west Europe: an archive of environmental change, uplift and early human occupation. Quaternary Science Reviews, 19, 1293-1303.

Bridgland, D.R., Westaway, R., 2008a. Climatically controlled river terrace staircases: A worldwide Quaternary phenomenon. Geomorphology, 98, 285-315.

Bridgland, D.R., Westaway, R., 2008b. Preservation patterns of Late Cenozoic fluvial deposits and their implications: results from IGCP 449. Quaternary International, 189, 5-38.

Broska, I., Petrík, I., 2015. Variscan thrusting in I- and S-type granitic rocks of the Tribeč Mountains, Western Carpathians (Slovakia): evidence from mineral compositions and monazite dating. Geologica Carpathica, 66, 6, 455—471.

Carslaw, H.S., Jaeger, J.C., 1959. Conduction of heat in solids, 2nd ed. Oxford University Press, Oxford.

Casas, I., De Pablo, J., Giménez, J., Torrero, M.E., Bruno, J., Cera, E., Finch, R.J., Ewing, R.C., 1998. The role of pe, pH, and carbonate on the solubility of UO_2 and uraninite under nominally reducing conditions. Geochimica et Cosmochimica Acta, 62, 2223–2231.

Čermák, V., 1977. Heat flow measured in five holes in eastern and central Slovakia. Earth and Planetary Science Letters, 34, 67-70.

Čermák, V., 1979. Review of heat flow measurements in Czechoslovakia. In: Čermák, V., Rybach, L., eds., Terrestrial heat Flow in Europe. Springer-Verlag, Berlin, pp. 152-160.

Černák, R., Remšík, A., Nádor, A., 2014. Geothermal energy research in Slovakia and cooperation on Geothermal Transboundary Project TRANSENERGY. Slovak Geological Magazine, 14 (2), 5-16.

Chernyshev, I.V., Konečný, V., Lexa, J., Kovalenker, V.A., Jeleň, S., Lebedev, V.A., Goltsman, Y.V., 2013. K-Ar and Rb-Sr geochronology and evolution of the Štiavnica stratovolcano (central Slovakia). Geologica Carpathica, 64 (4), 327-351.

Darulová, J., 2010. Banská Štiavnica: From localism to World Cultural Heritage. In: Bitušíková, A., Luther, D., eds., Cultural and Social Diversity in Slovakia III: Global and Local in a Contemporary City. Institute of Social and Cultural Studies, Matej Bel University, Banská Bystrica, pp. 81-88.

Dérerová, J., Zeyen, H., Bielik, M., Salman, K., 2006. Application of integrated geophysical modeling for determination of the continental lithospheric thermal structure in the eastern Carpathians. Tectonics, 25, TC3009, 12 pp. doi: 10.1029/2005TC001883

Dong, G., Morrison, G.W., 1995. Adularia in epithermal veins, Queensland: morphology, structural state and origin. Mineralium Deposita, 30, 11-19.

Drew, L.J., 2006. A tectonic model for the spatial occurrence of porphyry copper and polymetallic vein deposits—Applications to central Europe. U.S. Geological Survey Scientific Investigations Report 2005–5272, 36 p.

Elless, M.P., Lee, S.Y., 1998. Uranium solubility of carbonate-rich uranium-contaminated soils. Water, Air, and Soil Pollution, 107, 147-162.

Feely, M., Madden, J.S., 1987. The spatial distribution of K, U, Th and surface heat production in the Galway Granite, Connemara, western Ireland. Irish Journal of Earth Sciences, 8, 155-164.

Fendek, M., Bágelová, A., Fendeková, M., 2011. Geothermal energy world-wide and in Slovakia. Podzemná Voda, 17 (1), 74-83 (in Slovak with English abstract).

Fendek, M., Fendeková, M., 2005. Country Update of the Slovak Republic. In: Proceedings World Geothermal Congress 2005, Antalya, Turkey, 24-29 April 2005, paper 0173, 9 pp. Available online: http://www.geothermal-energy.org/pdf/IGAstandard/WGC/2005/0173.pdf (accessed 23 July 2016)

Fendek, M., Fendeková, M., 2015. Country Update of the Slovak Republic. In: Proceedings World Geothermal Congress 2015, Melbourne, Australia, 19-25 April 2015, paper 01060, 8 pp. Available online: https://pangea.stanford.edu/ERE/db/WGC/papers/WGC/2015/01060.pdf (accessed 29 June 2016)

Fendek, M., Rebro, A., Fendeková, M., 1999. A spell cast: historical aspects of thermal spring use in the Western Carpathian Region. In: Cataldi, R., Hodgson, S., Lund, J.W. Eds., Stories from a heated Earth. Geothermal Resources Council, Sacramento, California, pp. 251-264. ISBN 0-934412-19-7.

Fodor, L., Jelen B., Márton, M., Skaberne, D., Čar, J., Vrabec M., 1998. Miocene-Pliocene tectonic evolution of the Slovenian Periadriatic fault: Implications for Alpine-Carpathian extrusion models. Tectonics, 17, 690–709.

Franko, O., Remšík, A., Fendek, M., 1995. Atlas of Geothermal Energy in Slovakia. Dionýz Štúr Institute of Geology, Bratislava.

Fričovský, B., Černák, R., Marcin, D., Benková, K., Remšík, A., Fendek, M., 2016. Engineering approach in classification of geothermal resources of the Slovak Republic (western Carpathians). In: Proceedings, 41st Workshop on Geothermal Reservoir Engineering, Stanford University, Stanford, California, 22-24 February 2016. Paper SGP-TR-209, 10 pp. Available online: https://pangea.stanford.edu/ERE/db/GeoConf/papers/SGW/2016/Fricovsky.pdf (accessed 28 June 2016)

Fričovský, B., Jacko Jr., S., Chytilová, M., Tometz, L., 2012. Geothermal energy of Slovakia - CO_2 emissions reduction contribution potential (background study for conservative and non-conservative approach). Acta Montanistica Slovaca, 17, (4), 290-299.

Gorman-Lewis, D., Burns, P.C., Fein, J.B., 2008. Review of uranyl mineral solubility measurements. Journal of Chemical Thermodynamics, 40, 335–352

Handy, M.R., Ustaszewski, K., Kissling, E., 2014. Reconstructing the Alps–Carpathians–Dinarides as a key to understanding switches in subduction polarity, slab gaps and surface motion. International Journal of Earth Sciences (Geologische Rundschau), 104, 1-26.

Harangi, S., Downes, H., Thirlwall, M., Gméling, K., 2007. Geochemistry, petrogenesis and geodynamic relationships of Miocene calc-alkaline volcanic rocks in the Western Carpathian arc, eastern Central Europe. Journal of Petrology, 48, 2261-2287.

Herčko, P., Domaracká, L., Ambroš, P., 2014. Mining Bethlehem at Banská Štiavnica - example of mining heritage in Slovakia. Acta Geoturistica, 5 (2), 64-68.

Horváth, F., Musitz, B., Balázs, A., Végh, A., Uhrin, A., Nádor, A., Koroknai, B., Pap, N., Tóth, T., Wórum, G., 2015. Evolution of the Pannonian Basin and its geothermal resources. Geothermics, 53, 328–352.

Hrouda, F., Plašienka, D., Gregorová, D., 2002. Assumed Neogene deformation in the central Western Carpathians as inferred from magnetic anisotropy investigations. European Geosciences Union Stephan Mueller Special Publication Series, 1, 125–136.

Hudáček, M., Kubičková, J., 2005. Quantity and quality of the mine waters in Central Slovak Neovolcanic Mountains according to actual legislation. Podzemná Voda, 11 (1), 113-123 (in Slovak with English abstract).

Hurst, M.D., Mudd, S.M., Attal, M., Hilley, G., 2013. Hillslopes record the growth and decay of landscapes. Science, 341, 868-871.

Husák, L., Král, M., 1984. Radioaktivita hornín a zemský tepelný tok vo vybraných oblastiach Západných Karpá. In: Kapička, A., ed., Sborník fyzikálni vlastnosti hornín a jejich využití v geofyzice a geológii. Proceedings of the March 1984 conference, Liblice, Czechoslovakia. Union of Czechoslovak Mathematicians and Physicists, Prague, 186 pp.

Husák, Ľ., Král, M., 1986. Podiel rádioaktivity hornín Západných Karpát na tepelnom toku. In: Proceedings of the 'Geotermálna energia Slovenska a jej využitie' conference, Bratislava, 29 March 1984. Dionýz Štúr Geological Institute, Bratislava, pp. 31-37.

IAEA, 2003. Guidelines for radioelement mapping using gamma ray spectrometry data. Report IAEA-TECDOC-1363. International Atomic Energy Agency, Vienna, 173 pp. Available online: www-pub.iaea.org/mtcd/publications/pdf/te_1363_web.pdf (accessed 16 July 2016)

IAEA, 2010. Radioelement mapping. Report IAEA-NF-T-1.3. International Atomic Energy Agency, Vienna, 108 pp. Available online: www-pub.iaea.org/MTCD/Publications/PDF/Pub1463_web.pdf (accessed 10 December 2016)

Karsten, I., 2015. Banské, technické, a iné pamiatky. http://karstenivan.blogspot.co.uk/2015/10/banicke-myty-historicka-skutocnost.html (accessed 23 July 2016)

Kodera, P., Lexa, J., Rankin, A.H., Fallick, A.E., 2004. Fluid evolution in a subvolcanic granodiorite pluton related to Fe and Pb-Zn mineralization, Banská Štiavnica ore district, Slovakia. Economic Geology, 99, 1745–1770.

Kodera, P., Lexa, J., Fallick, A.E., Wälle, M., Biroň, A., 2014. Hydrothermal fluids in epithermal and porphyry Au deposits in the Central Slovakia Volcanic Field. In: Garofalo, P.S., Ridley, J.R. (eds), Gold-Transporting Hydrothermal Fluids in the Earth's Crust. Geological Society, London, Special Publications, 402, 177–206.

Kodera, P., Rankin, A.H., Fallick, A.E., 2001. Fluid processes in intrusion-related Pb-Zn stockworks (Štiavnica-Hodruša ore district, Slovakia). In: Piestrzynski, A., ed., Mineral deposits at the beginning of the 21st century. Swets & Zeitlinger, Lisse, the Netherlands, pp. 531-534.

Konečný, V., 1971. Evolutionary stages of the Banská Štiavnica caldera and its post-volcanic structures. Bulletin Volcanologique, 35, 95-116.

Konečný, V., Lexa, J., 2001. Structure and evolution of the Štiavnica Stratovolcano. Mineralia Slovaca 33, 179-196 (in Slovak).

Konečný, V., Lexa, J., Balogh, K., 1999. Neogene-Quaternary alkali basalt volcanism in central and southern Slovakia (Western Carpathians). Geolines, 9, 67-75.

Kováč, M., Nagymarosy, A., Soták, J., Šutovská, K., 1993. Late Tertiary paleogeographic evolution of the West Carpathians. Tectonophysics, 226, 401-416.

Kováč, M., Kráľ, J., Márton, E. Plašienka, D., Uher, P., 1994. Alpine uplift history of the central Western Carpathians: geochronological, paleomagnetic, sedimentary and structural data. Geologica Carpathica, 45, 83-96.

Lachenbruch, A.H., 1970. Crustal temperature and heat production: Implications of the linear heat-flow relation. Journal of Geophysical Research, 75, 3291-3300.

Lee, M.K., Brown, G.C., Webb, P.C., Wheildon, J., Rollin, K.E., 1987. Heat flow, heat production and thermo-tectonic setting in mainland UK. Journal of the Geological Society, London, 144, 35–42.

Lexa, J., Štohl, J., Konečný, V., 1999. The Banská Štiavnica ore district: relationship between metallogenetic processes and the geological evolution of a stratovolcano. Mineralium Deposita, 34, 639–654.

Lizoň, I., 1975. Niektoré výsledky geotermických vyskumov v západných Karpatoch. In: Proceedings of the 6th National Geophysics Conference, Plzeň, Czechoslovakia, pp. 477-495.

Løvborg, L., 1984. The calibration of portable and airborne gamma-ray spectrometers - theory, problems, and facilities. Report no. 2456, Risø National Laboratory, Roskilde, Denmark, 207 pp. Available online: www.qsl.net/k0ff/016%20Manuals/Geometrics/GR410%20setup.pdf (accessed 9 July 2016)

Luikov, A.V., 1968. Analytical heat diffusion theory. Academic Press, New York.

McCay, A.T., 2016. Heat production measurements from Scottish granites. Available online: http://researchdata.gla.ac.uk/id/eprint/302 (accessed 31 December 2016)

McCay, A.T., Harley, T.L., Younger, P.L., Sanderson, D.C.W., Cresswell, A.J., 2014. Gamma-ray spectrometry in geothermal exploration: state of the art techniques. Energies, 7, 4757-4780.

Miles, A., Graham, C., Hawkesworth, C., Gillespie, M., Dhuime, B., Hinton, R., 2014. Using zircon isotope compositions to constrain crustal structure and pluton evolution: the Iapetus Suture Zone granites in northern Britain. Journal of Petrology, 55, 181-207.

Nemčok, M., Konečny, P., Lexa, O., 2000. Calculations of tectonic, magmatic and residual stress in the Štiavnica stratovolcano, western Carpathians: implications for mineral precipitation paths. Geologica Carpathica, 51, 19-36.

Pavolová, H., Čulková, K., Bakalár, T., 2010. Utilization of geothermal energy in Slovakia. Acta Montanistica Slovaca, 20 (4), 326-333

Plašienka, D., Grecula, P., Putiš, M., Kováč, M., Hovorka, D., 1997. Evolution and structure of the Western Carpathians: an overview. In: Grecula, P., Hovorka, D., Putiš, M. (Eds.), Geological Evolution of the Western Carpathians. Mineralia Slovaca - Monograph, Bratislava, Slovakia, pp. 1 – 24.

Piller, W.E., Harzhauser, M., Mandic, O., 2007. Miocene Central Paratethys stratigraphy – current status and future directions. Stratigraphy, 4, (2/3), 151-168.

Recktenwald, G., 2013. Transient conduction in a sphere with convective boundary conditions. Available online: http://web.cecs.pdx.edu/~gerry/heatAnimations/sphereTransient/ (accessed 29 December 2016)

Remšík, A., Helma, J., Marcin, D., 2000. Niektoré poznatky o geotermálnych a minerálnych vodách v regióne Banská Štiavnica. Podzemná Voda, 6 (2), 93-101.

Remšík, A., Madar, D., Konečny, V., Král, M., Šefara, J., Grand, T., Weis, K., 2001. Geothermal waters of the Banska Štiavnica region and possibilities of their obtaining. Mineralia Slovaca, 33, 243-251 (in Slovak with English summary).

Remšík, A., Fendek, M., Bajo, I., Marcin, D., 2009. New results from the regional hydrogeothermal evaluation in Slovakia. In: Popovski, K., Vranovska, A., Popovska Vasilevska, S., Eds., Proceedings of the International Conference on National Development of Geothermal Energy Use and International Course / EGEC Business Seminar on Organization of Successful Development of a Geothermal Project, Častá Papiernička, Slovakia, 26-29 May 2009, 8 pp. Available online: www.geothermal-energy.org/pdf/IGAstandard/ISS/2009Slovakia/VIII.1Remsik.pdf (accessed 22 July 2016)

Rögl, F., 1996. Stratigraphic correlation of the Paratethys Oligocene and Miocene. Mitteilungen der Gesellschaft der Geologie- und Bergbaustudenten Österreichs, 41, 65-73.

Royden, L., Horváth, F., Rumpler, J., 1983. Evolution of the Pannonian Basin system. Tectonics, 2, 63–90.

Rybach, L., 1976. Radioactive heat production in rocks and its relation to other petrophysical parameters. Pure and Applied Geophysics, 114, 309-317.

Rybach, L., Buntebarth, G., 1981. Heat-generating radioelements in granitic magmas. Journal of Volcanology and Geothermal Research, 10, 395-404.

Rybach, L., Buntebarth, G., 1982. Relationships between the petrophysical properties density, seismic velocity, heat generation and mineralogical constitution. Earth and Planetary Science Letters, 57, 367-376.

Rybach, L., Buntebarth, G., 1984. The variation of heat generation, density and seismic velocity with rock type in the continental lithosphere. Tectonophysics, 103, 335-344.

Rybach, L., von Raumer, J., Adams, J.A.S., 1966. A gamma spectrometric study of Mont-Blanc granite samples Pure and Applied Geophysics, 63, 153-160.

Schmid, S.M., Fügenschuh, B., Kissling, E., Schuster, R., 2004. Tectonic map and overall architecture of the Alpine orogen. Eclogae geol. Helv. 97 (1), pp. 93–117.

Šefara, J., Bielik, M., 2009. Geofyzikálny obraz Západných Karpát a ich okolia: Geologická interpretácia geofyzikálnych meraní regionálneho a hlbinného charakteru. Comenius University, Bratislava, 173 pp. Available online: https://fns.uniba.sk/uploads/media/GeofObrazZK.pdf (accessed 3 March 2017)

Seghedi, L., Downes, H., 2011. Geochemistry and tectonic development of Cenozoic magmatism in the Carpathian–Pannonian region. Gondwana Research, 20, 655–672.

Šimon, L., Lexa, J., Konečný, V., 2002a. Pannonian basalt volcano Šibeničný Vrch, central Slovakia. In: Proceedings of the 17th Congress of the Carpathian-Balkan Geological Association, Bratislava, 1-4 September 2002. Geologica Carpathica, volume 53, Special Issue, 7 pp. Available online: http://www.geologicacarpathica.com/special-issues/53-2002/ (accessed 11 December 2016)

Šimon, L., Pauditš, P., Kráľ, J., 2002b. New data on the Putikov Vŕšok alkali basalt volcano, central Slovakia. In: Proceedings of the 17th Congress of the Carpathian-Balkan Geological Association, Bratislava, 1-4 September 2002. Geologica Carpathica, volume 53, Special Issue, 8 pp. Available online: http://www.geologicacarpathica.com/special-issues/53-2002/ (accessed 11 December 2016)

Smith, R.L., Bailey, R.A., Ross, C.S., 1961. Structural evolution of the Valles Caldera, New Mexico, and its bearing on the emplacement of ring dikes. U.S. Geological Survey Professional Paper 424-D, pp. 145-149.

Stampfli, G.M., Mosar, J., Favre, P.., Pillevuit A., Vannay, J.-C., 2001. Permo-Mesozoic evolution of the western Tethys realm: the Neo-Tethys East Mediterranean Basin connection. In: Ziegler, P.A., Cavazza, W., Robertson, A.H.F., Crasquin-Soleau, S. (Eds.), Peri-Tethys Memoir 6: Peri-Tethyan Rift/Wrench Basins and Passive Margins. Mémoires du Museum National d'Histoire Naturelle, Paris, 186, 51–108.

Stampfli, G.M., Von Raumer, J.F., Borel, G.D., 2002. Paleozoic evolution of pre-Variscan terranes: From Gondwana to the Variscan collision. In: Martínez Catalán, J.R., Hatcher, R.D., Jr., Arenas, R., Díaz García, F., eds., Variscan-Appalachian dynamics: The building of the late Paleozoic basement. Geological Society of America Special Paper 364, 263–280.

Stegena, L., Géczy, B., Horváth, F., 1975. Late Cenozoic evolution of the Pannonian Basin. Tectonophysics, 26, 71–90.

Steininger, F.F., Wessely G., 2000. From the Tethyan Ocean to the Paratethys Sea: Oligocene to Neogene Stratigraphy, Paleogeography and Paleobiogeography of the circum-Mediterranean region and the Oligocene to Neogene Basin evolution in Austria. Mitteilungen der Österreichischen Geologischen Gesellschaft, 92, 95-116.

Streckeisen, A., 1974. Classification and nomenclature of plutonic rocks recommendations of the IUGS subcommission on the systematics of igneous rocks. Geologische Rundschau, 63, 773-786.

Stüwe, K., White, L., Brown, R., 1994. The influence of eroding topography on steady-state isotherms: application to fission track analysis. Earth and Planetary Science Letters, 124, 63-74.

Šujan, M., Rybár, S., 2014. The development of Pleistocene river terraces in the eastern part of the Danube Basin. Acta Geologica Slovaca, 6 (2), 107–122 (in Slovak with English summary).

Szafián, P., Horváth, F., Cloetingh, S., 1997. Gravity constraints on the crustal structure and slab evolution along a Transcarpathian transect. Tectonophysics, 272, 233-247.

Szabo, C., Harangi, S., Csontos, L., 1992. Review of Neogene and Quaternary volcanism of the Carpathian-Pannonian region. Tectonophysics, 208, 243-256.

Tenzer, R., Sirguey, P., Rattenbury, M., Nicolson, J., 2011. A digital rock density map of New Zealand. Computers & Geosciences, 37, 1181-1191.

Tindle, A.G., Pearce, J.A., 1981. Petrogenetic modelling of in situ fractional crystallization in the zoned Loch Doon pluton, Scotland. Contributions to Mineralogy and Petrology, 78, 196–207.

UNESCO, 1993. Historic town of Banská Štiavnica and the technical monuments in its vicinity. Available online: http://whc.unesco.org/en/list/618 (accessed 25 June 2016)

Valderrama, I.M.P., Pérez-Pariente, J., 2012. Alchemy at the service of mining technology in seventeenth-century Europe, according to the works of Martine de Bertereau and Jean du Chastelet. Bulletin for the History of Chemistry, 37 (1), 1-13.

Vasiliev, I., Arjan de Leeuw, A., Filipescu, S., Krijgsman, W., Kuiper, K., Stoica, M., Briceag, A., 2010. The age of the Sarmatian–Pannonian transition in the Transylvanian Basin (Central Paratethys). Palaeogeography, Palaeoclimatology, Palaeoecology, 297, 54–69.

Veverka, B., 2004. Křovák's projection and its use for the Czech Republic and the Slovak Republic. In: Holota, P., Slaboch, V. (eds.), 50 years of the Research Institute of Geodesy, Topography and Cartography. Research Institute of Geodesy, Topography and Cartography, Prague, Czech Republic, pp. 173-179. Available online: https://web.archive.org/web/20150216143806/https://www.vugtk.cz/odis/sborniky/sb2005/Sbornik_50_let_VUGTK/Part_1-Scientific_Contribution/16-Veverka.pdf (accessed 21 June 2016)

Von Raumer, J.F., Stampfli, G.M., Borel, G., Bussy, F., 2002. The organization of pre-Variscan basement areas at the north-Gondwanan margin. International Journal of Earth Sciences, 91, 35–52.

Von Raumer, J.F., Stampfli, G.M., Bussy. B., 2003. Gondwana-derived microcontinents? The constituents of the Variscan and Alpine collisional orogens. Tectonophysics, 365, 7-22.

Vozárová, A., Ebner, F., Kovács, S., Kräutner, H.-G., Szederkenyi, T., Krstić, B., Sremac, J., Aljinovič, D., Novak, M., Skaberne, D., 2009. Late Variscan Carboniferous to Permian) environments in the Circum Pannonian Region. Geologica Carpathica, 60, 71—104.

Westaway, R., 1998. Dependence of active normal fault dips on lower-crustal flow regimes. Journal of the Geological Society, London, 155, 233–253.

Westaway, R., 2002. The Quaternary evolution of the Gulf of Corinth, central Greece: coupling between surface processes and flow in the lower continental crust. Tectonophysics, 348, 269–318.

Westaway, R., Bridgland, D.R., 2014. Relation between alternations of uplift and subsidence revealed by Late Cenozoic fluvial sequences and physical properties of the continental crust. Boreas, 43, 505–527.

Westaway, R., Bridgland, D.R., Sinha, R., Demir, T., 2009. Fluvial sequences as evidence for landscape and climatic evolution in the Late Cenozoic: a synthesis of data from IGCP 518. Global and Planetary Change, 68, 237–253.

Zeyen, H., Dérerová, J., Bielik, M., 2002. Determination of the continental lithospheric thermal structure in the Western Carpathians: integrated modelling of surface heat flow, gravity anomalies and topography. Physics of the Earth and Planetary Interiors, 134, 89-104.

Table 1: Cermak (1979) heat flow data – on a separate sheet

Table 2: Franko et al. (1995) heat flow data – on a separate sheet

Table 3: Heat production measurements – on a separate sheet

Table 4: Comparison of estimates of composition

	This study			Chernyshev et al. (2013)	
Lithology	N	[K] (1) (wt%)	[K_2O] (2) (wt%)	N	[K_2O] (3) (wt%)
Brehy basalt	1	1.78	2.14	3	1.64±0.76
Studenec Formation andesitic lava	3	2.30±1.59	2.77±1.92	3	2.67±0.40
Štiavnica diorite	3	4.52±4.51	5.44±5.43	1	1.52
Štiavnica granodiorite	15	6.02±3.27	7.25±3.94	2	3.54±0.06

N denotes the number of samples analyzed, each gamma ray spectrometry sample consisting of three separate measurements as described in the text. For N>1 the margins of uncertainty are expressed as ±2σ.

Notes:

(1)...mean value from portable gamma-ray spectrometer measurements, expressed ±2σ.

(2)...mean value derived from portable gamma-ray spectrometer measurements, scaled as discussed in the text to convert to percentage by weight of K_2O, also expressed ±2σ.

(3)...value determined by geochemical analysis (Chernyshev et al., 2013), again expressed ±2σ.

Figure captions

Figure 1. Map of western and central Slovakia, showing the study region and surrounding localities discussed in the text. Inset shows location within Europe.

Figure 2. Map illustrating the Carpathian Arc encompassing the Pannonian Basin, modified from Fig. 2(a) of Chernyshev et al. (2013). The Carpathian Arc is delineated by the Carpathian accretionary prism, which in the Western Carpathians follows the borders between Slovakia and the Czech Republic and Slovakia and Poland, to the north (Fig. 1). The Internal Carpathian structural units depicted include the AlCaPa Block, bounded to the south by the Mid-Hungarian Fault Zone (emboldened), and including the sutured remains of ancient terranes such as the Tatra-Fatra Belt and Vepor Belt (see the main text).

Figure 3. Simplified summary map of the Late Cenozoic magmatic activity in the Central Slovakian Volcanic Field, modified from Fig. 2(b) of Chernyshev et al. (2013). Phases of magmatism are numbered to match the presentation of our heat production results in Table 3. As regards 'phase 0', the (? pre-) Variscan basement, the large outcrop around Podkriváň is depicted east of the Javorie upland, whereas the smaller inliers around Lieskovec and Vyhne are also depicted, respectively east of Zvolen and NW of Banská Štiavnica. The Šibeničný Vrch neck east of Žiar nad Hronom, which is mentioned in the text as a constituent of the Late Miocene phase of basaltic andesite volcanism is labelled S. 'Phase 6', the youngest phase of alkali basalt eruption, is depicted at Brehy near Nová Baňa (labelled B), Ostrá Lúka SW of Zvolen (labelled O), Rakovec (labelled R), and at the Kalvária and Kyhisýbel necks east of Banská Štiavnica (jointly labelled K: the former circa UTM co-ordinates CU 45810 69734 and Křovák co-ordinates -437105 -1257568; the latter farther east, circa CU 47557 69606 and -435366 -1257783).

Figure 4. Map of the same region as in Fig. 1, showing contours of surface heat flow at 10 mW m^{-2} intervals, with local maxima and minima marked by + and – symbols and areas with heat flow >100 mW m^{-2} and <50 mW m^{-2} shaded for emphasis. Note the maximum values of >100 mW m^{-2} in the vicinity of Banská Štiavnica (cf. Fig. 1). Modified from Fig. 2 of Fričovský et al. (2016), based originally on Franko et al. (1995).

Figure 5. Excerpt from colour-shaded Bouguer gravity anomaly map covering central-southern Slovakia, from the http://mapserver.geology.sk/gravimetria/ online system. The Křovák co-ordinate grid (in km) provides scale; the top right corner is near Liptovský Mikuláš (Fig. 1) and the bottom centre is on the border between Slovakia and Hungary near Šahy. Crosses (+) mark the positions of Banská Štiavnica and Vigľašská Huta – Kalinka, near the centres of Middle Miocene granitic intrusions. See text for discussion.

Figure 6. (a) Simplified map of the geology and hydrogeology in the central part of the Štiavnica upland. This map is modified from Fig. 1 of Remšík et al. (2000), with the addition of mine drainage adits using information from Bajtoš (2001), Hudáček and Kubičková (2005), and Karsten (2015). Discharge occurs from many more mine drainage adits in this region (see Hudáček and Kubičková, 2005, for details); those depicted have the largest discharge (Voznícka, 200 l s^{-1}; Nová Voznícka, 50 l s^{-1}; Richňava, 50 l s^{-1}; Kreutzerfindung, 11 l s^{-1}; Hoffer, 8 l s^{-1}; and Zlatý Stôl, 8 l s^{-1}). The geology illustrated, which is excerpted from mapping dating back to 1984, differs somewhat from its modern representations in the online mapping (see Fig. 7) and by Chernyshev et al. (2013) (see Fig. 3). The principal normal faults depicted, which strike southward between Hodruša-Hámre and Vyhne, southwestward between Vyhne and Sklené Teplice, and northward between Sklené Teplice and Banská Štiavnica, delineate the 'resurgent horst' in modern interpretations (cf. Fig. 3). However, the Štiavnica pluton, which crops out across much of this 'resurgent horst' (Fig. 7), has been completely omitted from this depiction. (b) Map, modified after Franko et al. (1995), of the central part of the study region, using geographical co-ordinates, showing locations of boreholes that provided the geothermal data in Table 2. (c) Map of roughly the same area as in (b), showing Bouguer gravity anomalies (in mgal), from the http://mapserver.geology.sk/gravimetria/ online system. This map is indexed to the Křovák co-ordinate system; the co-ordinate grid (in km) provides scale. Placenames are indicated thus: B, Banky; BB, Banská Belá; BS, Banská Štiavnica; BSt, Bansky Studenec; D, Dekýš; H, Hliník nad Hronom; HH, Hodrušá Hámre; K, Kopanice; N, Nová Baňa; P, Pukanec; Ph, Podhorie; Po, Počúvadlo; SB, Štiavnicé Bane ; ST, Sklené Teplice; V, Vyhne; Va, Vysoká; Z, Žarnovica; ZH, Žiar nad Hronom (railway station). Note (cf. Fig. 3) the concentric circular pattern indicating the gravity high in the resurgent horst surrounded by the gravity low in the caldera.

Figure 7. Simplified geological map of the central part of the study region, based on the 1:25,000 scale mapping from http://mapserver.geology.sk/gm50js/, showing heat-production measurement sites in

relation to outcrop of the Štiavnica pluton. Kl denotes the location of the Klinger Kratka mine adit (cf. Fig. 6(a) and Table 1). The key includes codes used to label each Formation in the geological mapping.

Figure 8. Map showing results for the whole study region. (a) Classification of samples. (b) Heat production.

Figure 9. Map showing results for the Štiavnica upland. (a) Classification of samples, using the same format as Fig. 8(a). (b) Heat production, using the same format as Fig. 8(b).

Figure 10. Graphs of predicted temperature (a) and geothermal gradient (b) for various hypotheses, assumed to involve steady-state conditions, representing the present-day thermal state of the Štiavnica upland. All solutions assume a Moho depth of 34 km, consistent with Franko et al. (1995), a surface temperature of 8 °C, and a thermal diffusivity of 1.2 $mm^2 s^{-1}$. Solution 1 is for uniform heat production 5 $\mu W m^{-3}$ across the uppermost 8 km of the crust and zero heat production elsewhere. Solution 2 is for heat production at the Earth's surface Y_o=5 $\mu W m^{-3}$, decreasing downward exponentially with a scale depth D=8 km. Theory for these solutions has been published many times (e.g., Lachenbruch, 1970; Westaway and Bridgland, 2014); in both cases, basal heat flow of 70 $mW m^{-2}$ is assumed. Solution 3 is for steady-state erosion at a rate U=1.39 $mm a^{-1}$, with temperature being maintained at a steady basal temperature T_b=700 °C at 32 km depth. Theory for this solution has bene published by Stüwe et al. (1994) and Westaway (2002). This 32 km depth is adopted (here and for solutions 4 and 5) based on the assumption that isostatic compensation is maintened by lower-crustal flow subject given the Moho depth and crustal thermal state (cf. Westaway, 1998). Solution 4 assumes a combination of erosion and radioactive heat production with Y_o=5 $\mu W m^{-3}$, D=4 km, U=0.96 $mm a^{-1}$, and T_b=650 °C at 32 km depth; solution 5 assumes the samevalues of Y_o and T_b, with D=8 km and U=0.32 $mm a^{-1}$. All solutions give the same geothermal gradient, 36.7 °C km^{-1} at the Earth's surface, consistent with surface heat flow 110 $mW m^{-2}$ for a thermal conductivity of 3 $W m^{-1} °C^{-1}$. See text for discussion.

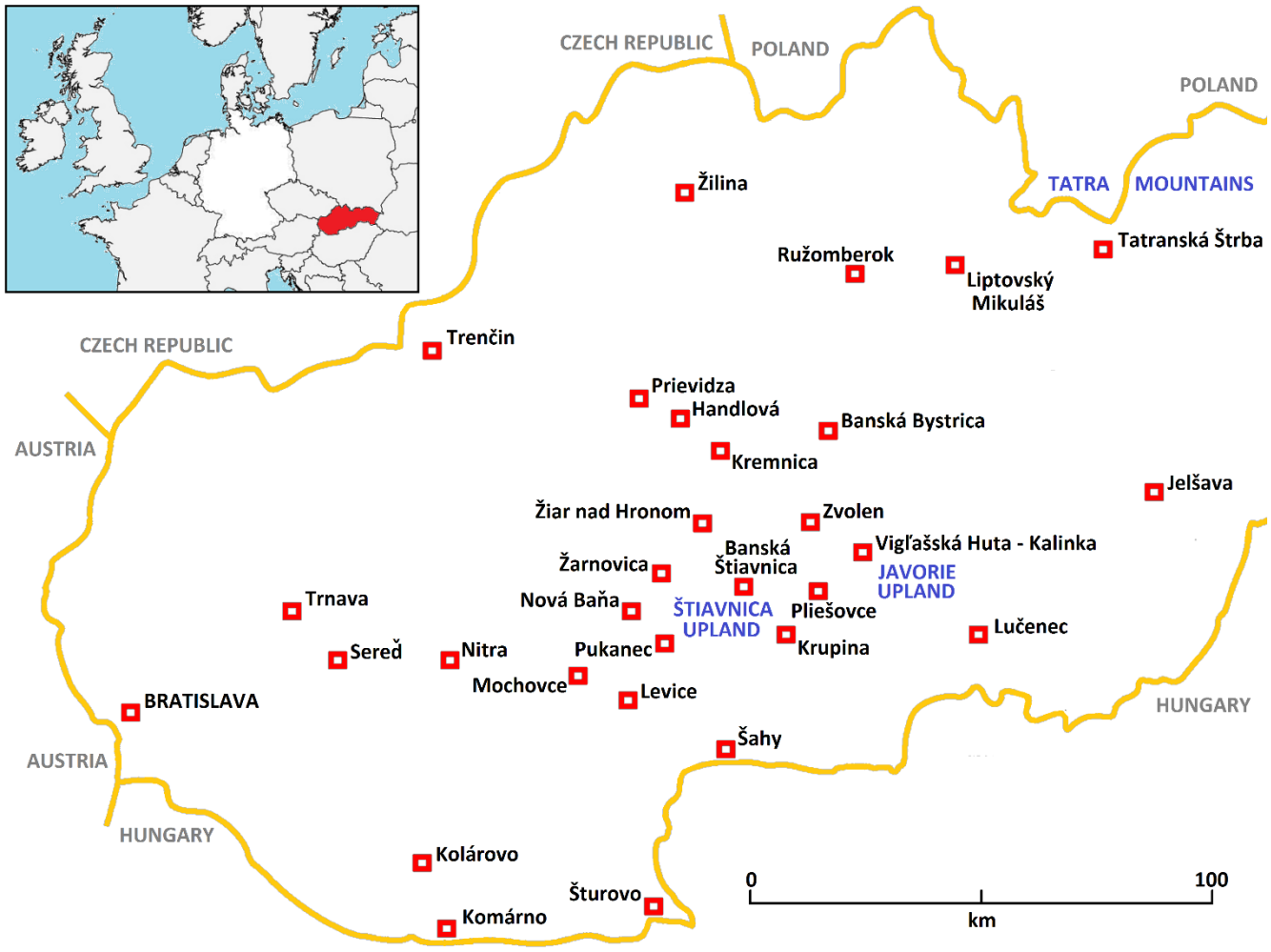
CZECH REPUBLIC
POLAND
POLAND
Žilina
TATRA
MOUNTAINS
Tatranská Štrba
Ružomberok
Liptovský
Mikuláš
CZECH REPUBLIC
Trenčin
Prievidza
Handlová
Banská Bystrica
AUSTRIA
Kremnica
Jelšava
Žiar nad Hronom
Zvolen
Vigľašská Huta - Kalinka
Banská
Štiavnica
Žarnovica
JAVORIE
UPLAND
Trnava
Nová Baňa
ŠTIAVNICA
UPLAND
Pliešovce
Lučenec
Sereď
Nitra
Pukanec
Krupina
Mochovce
Levice
BRATISLAVA
HUNGARY
Šahy
AUSTRIA
HUNGARY
Kolárovo
Šturovo
Komárno
0
100
km

Figure 1

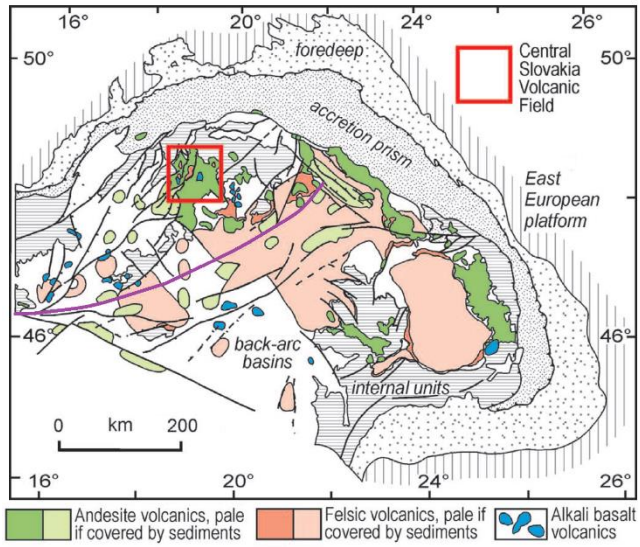
16°
20°
24°
26°
50°
46°
foredeep
accretion prism
Central
Slovakia
Volcanic
Field
East
European
platform
back-arc
basins
internal units
0
km
200
Andesite volcanics, pale if covered by sediments
Felsic volcanics, pale if covered by sediments
Alkali basalt volcanics

Figure 2

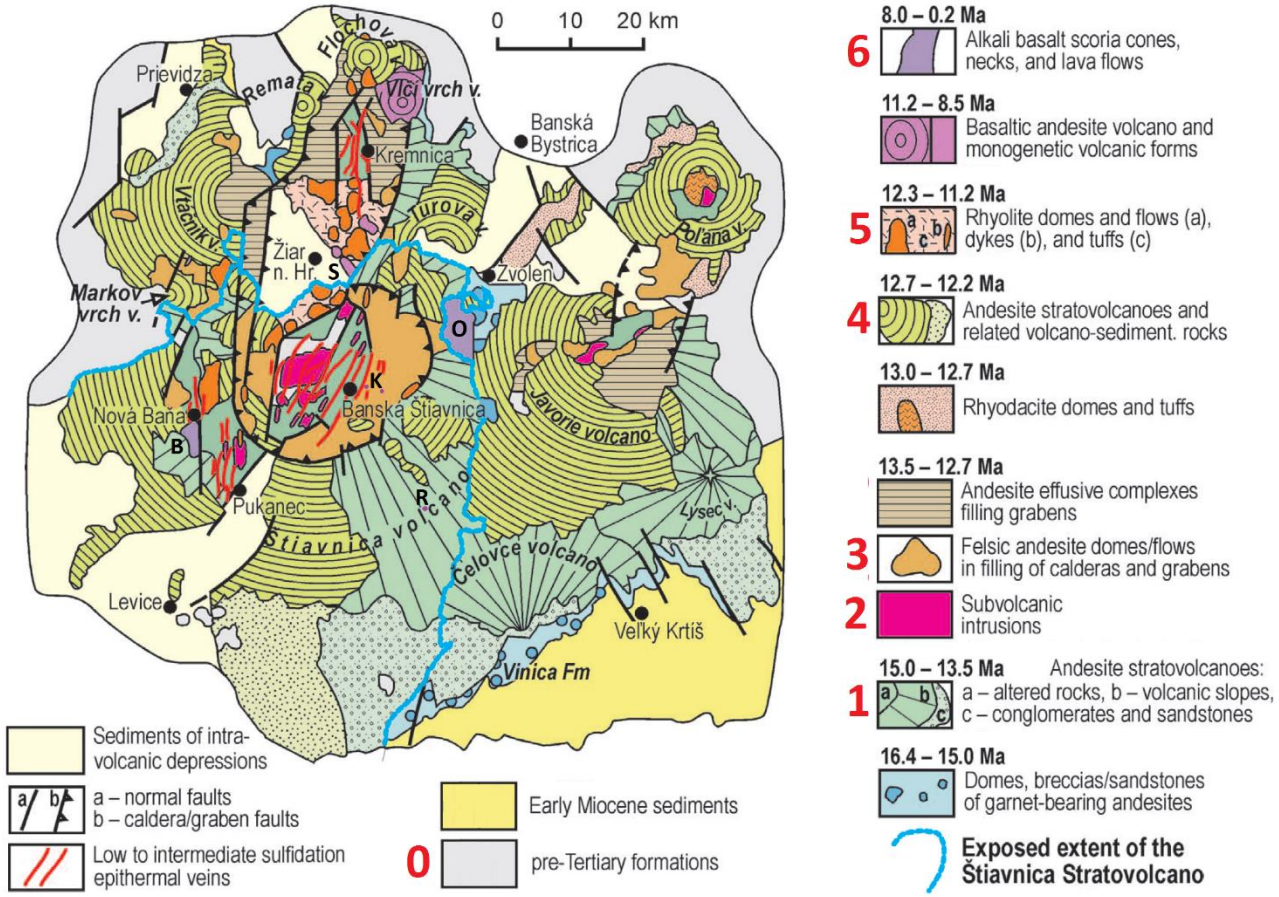
0 10 20 km
Prievidza
Remata
Vlčí vrch v.
Banská Bystrica
Kremnica
Vtáčnik v.
Turová v.
Poľana v.
Žiar n. Hr.
S
Zvolen
Markov vrch v.
O
K
Nová Baňa
Banská Štiavnica
Javorie volcano
B
R
Pukanec
Štiavnica volcano
Lysec v.
Čelovce volcano
Levice
Veľký Krtíš
Vinica Fm
Sediments of intra-volcanic depressions
a – normal faults
b – caldera/graben faults
Low to intermediate sulfidation epithermal veins
Early Miocene sediments
0
pre-Tertiary formations
8.0 – 0.2 Ma
6
Alkali basalt scoria cones, necks, and lava flows
11.2 – 8.5 Ma
Basaltic andesite volcano and monogenetic volcanic forms
12.3 – 11.2 Ma
5
Rhyolite domes and flows (a), dykes (b), and tuffs (c)
12.7 – 12.2 Ma
4
Andesite stratovolcanoes and related volcano-sediment. rocks
13.0 – 12.7 Ma
Rhyodacite domes and tuffs
13.5 – 12.7 Ma
Andesite effusive complexes filling grabens
3
Felsic andesite domes/flows in filling of calderas and grabens
2
Subvolcanic intrusions
15.0 – 13.5 Ma
Andesite stratovolcanoes:
1
a – altered rocks, b – volcanic slopes, c – conglomerates and sandstones
16.4 – 15.0 Ma
Domes, breccias/sandstones of garnet-bearing andesites
Exposed extent of the Štiavnica Stratovolcano

Figure 3

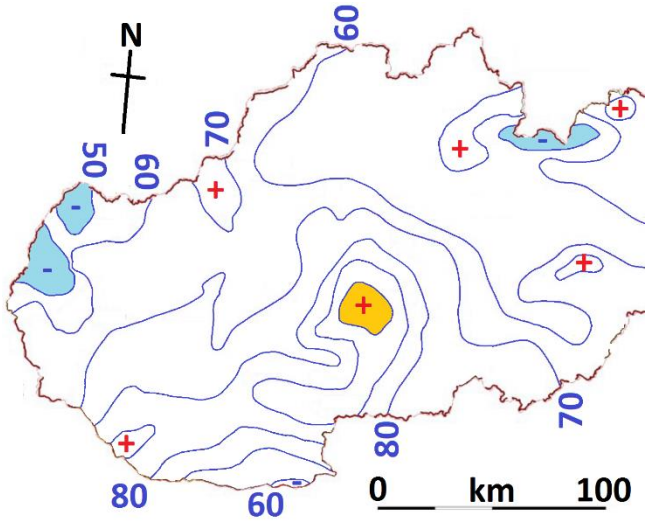

Figure 4

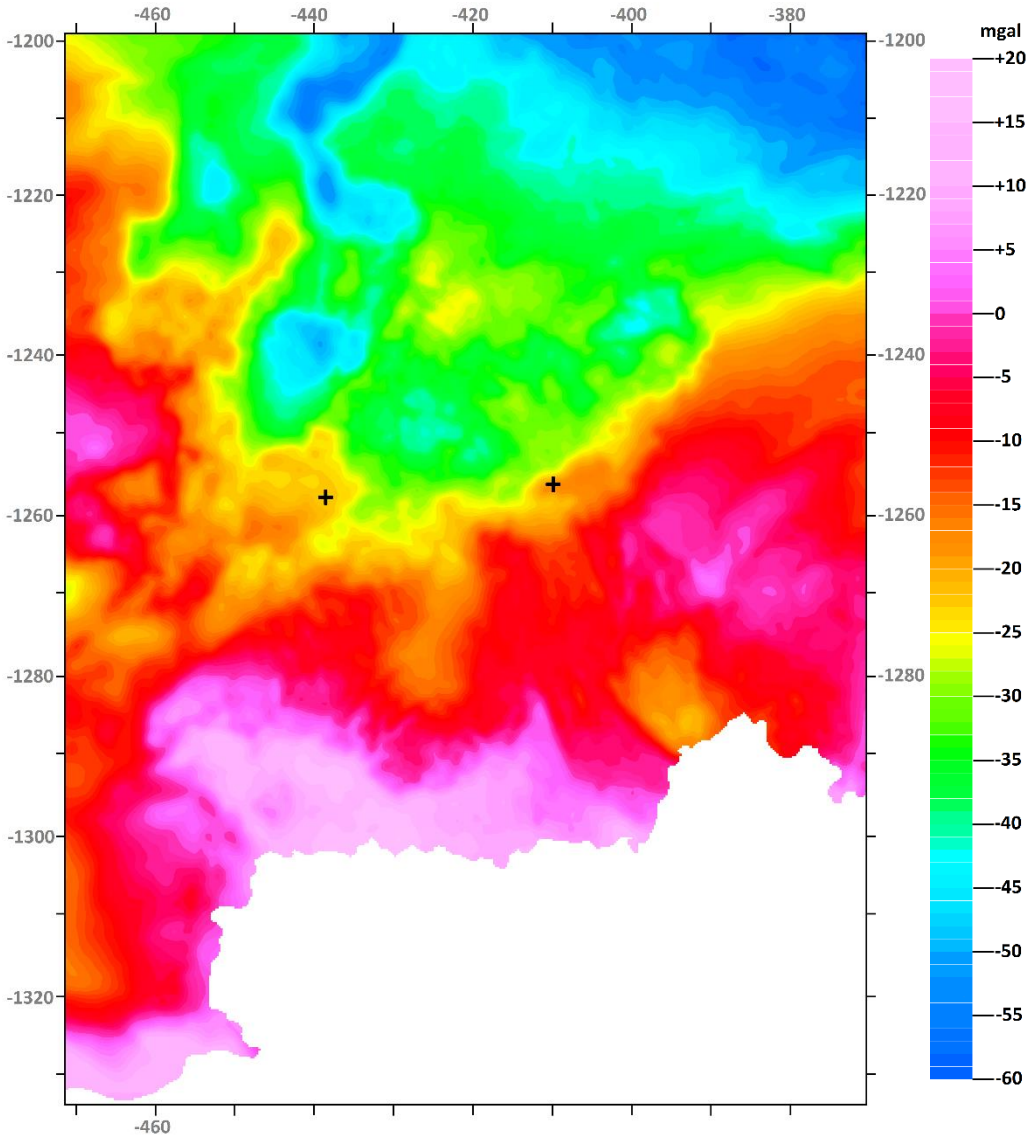
-460
-440
-420
-400
-380
-1200
-1220
-1240
-1260
-1280
-1300
-1320
mgal
+20
+15
+10
+5
0
-5
-10
-15
-20
-25
-30
-35
-40
-45
-50
-55
-60

Figure 5

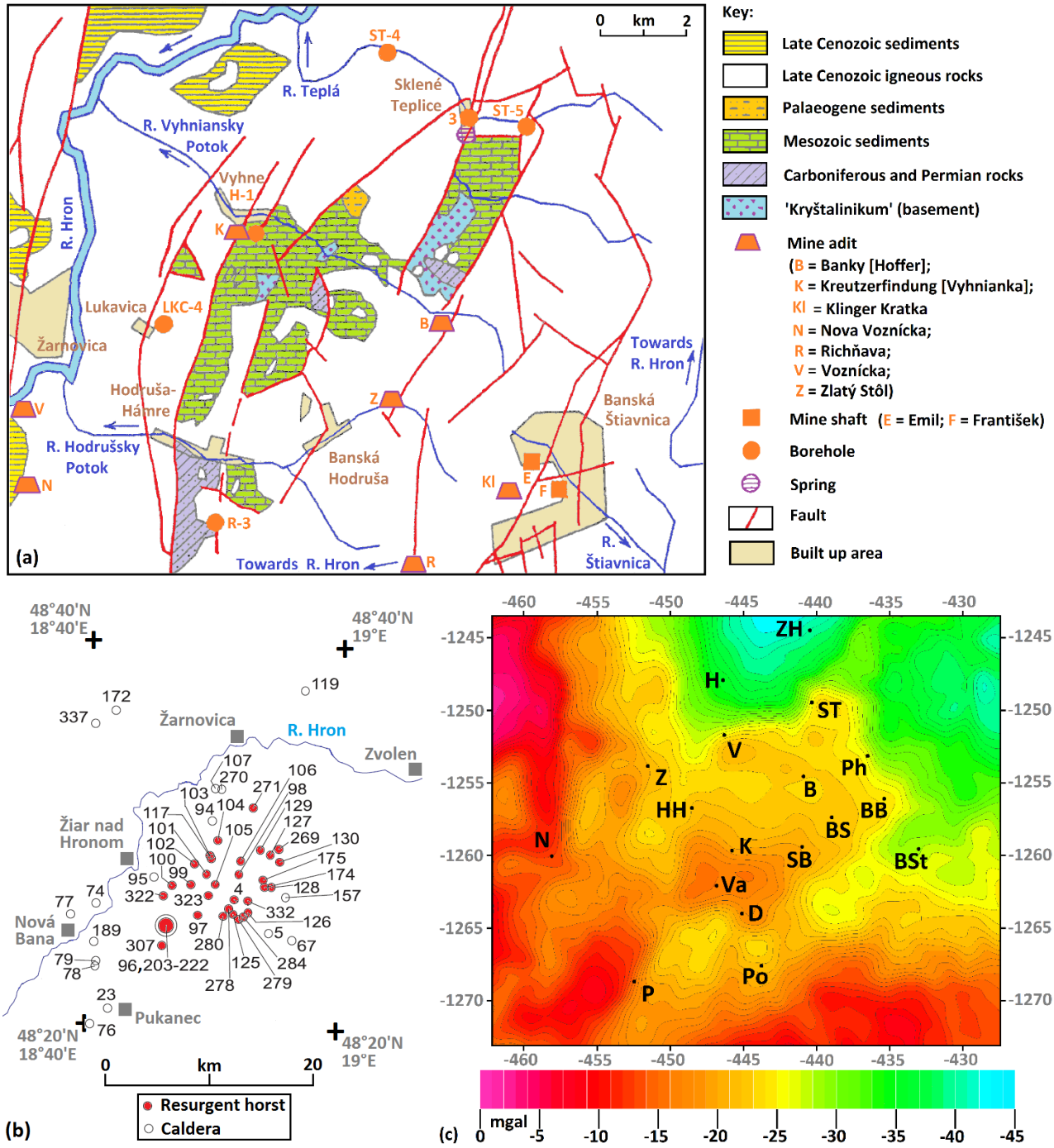
0 km 2
ST-4
R. Teplá
Sklené Teplice
ST-5
3
R. Vyhniansky Potok
Vyhne
H-1
K
R. Hron
Lukavica
LKC-4
Žarnovica
B
Towards R. Hron
Hodruša-Hámre
V
Z
Banská Štiavnica
R. Hodrušský Potok
N
Banská Hodruša
Kl
E
F
R-3
(a)
Towards R. Hron
R
R. Štiavnica
Key:
Late Cenozoic sediments
Late Cenozoic igneous rocks
Palaeogene sediments
Mesozoic sediments
Carboniferous and Permian rocks
'Kryštalinikum' (basement)
Mine adit
(B = Banky [Hoffer];
K = Kreutzerfindung [Vyhnianka];
Kl = Klinger Kratka
N = Nova Voznícka;
R = Richňava;
V = Voznícka;
Z = Zlatý Stôl)
Mine shaft (E = Emil; F = František)
Borehole
Spring
Fault
Built up area
48°40'N 18°40'E
48°40'N 19°E
48°20'N 18°40'E
48°20'N 19°E
Žarnovica
R. Hron
Zvolen
Žiar nad Hronom
Nová Baňa
Pukanec
0 km 20
Resurgent horst
Caldera
(b)
-460 -455 -450 -445 -440 -435 -430
-1245
-1250
-1255
-1260
-1265
-1270
ZH
H
ST
V
Z
Ph
B
HH
BB
BS
N
K
SB
BSt
Va
D
Po
P
mgal 0 -5 -10 -15 -20 -25 -30 -35 -40 -45
(c)

Figure 6

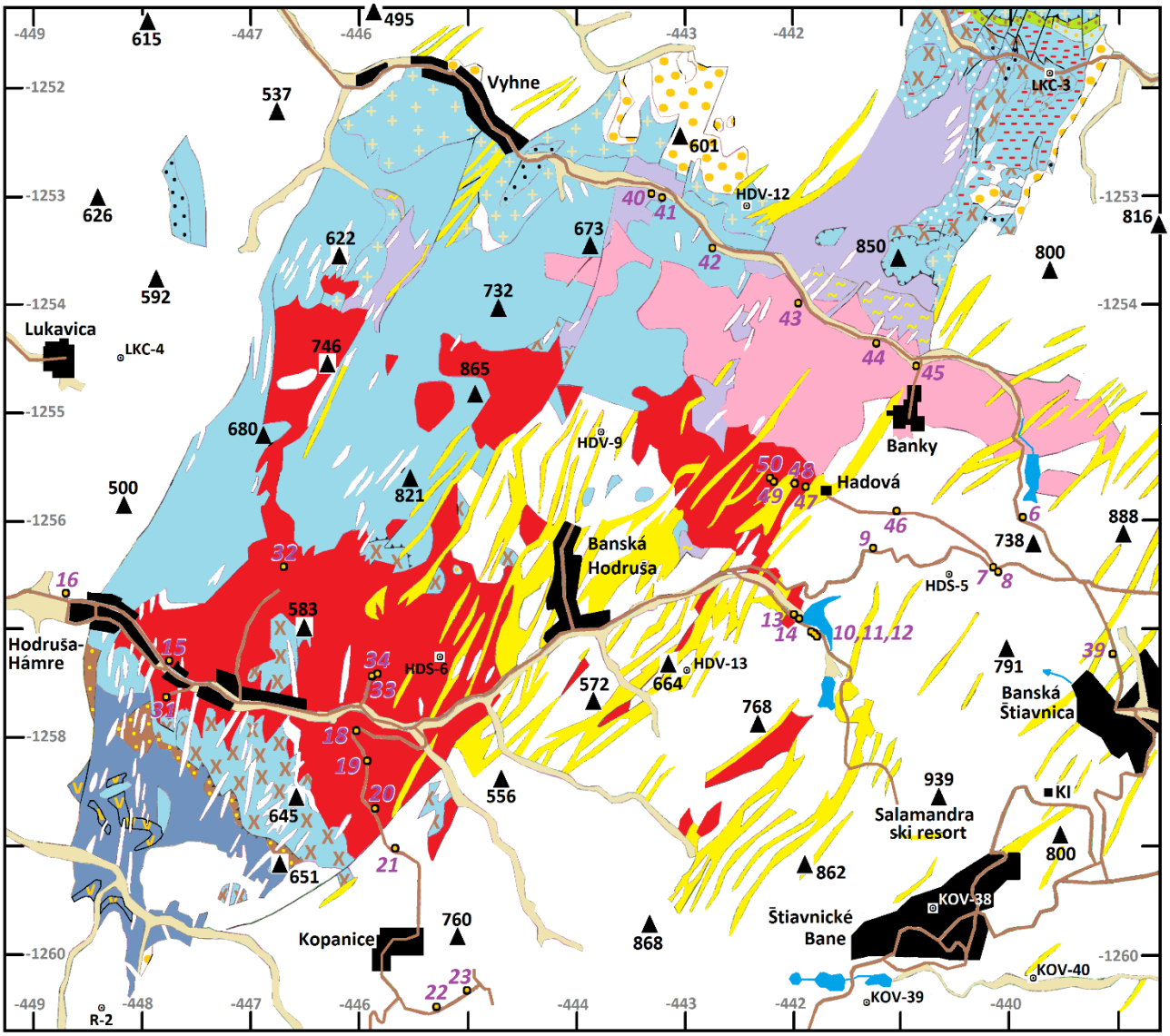

Key:

- Sample site
- Borehole
- Spot height in metres
- Mine reservoir
- Holocene floodplain alluvium
- Miocene 'argillite' (m3)
- Štiavnica pluton - granodiorite (Si8BS)
- Štiavnica pluton - diorite (Si9BS)
- Other Miocene igneous rocks
- Palaeogene clastic sediment (Borovsk Fm.) (Bo)
- Cretaceous clastic sediment (Poruba Fm.) (PoK12)
- Jurassic limestone and chert (Ždiarske Fm.) (ZdJ23)
- Triassic sandstone (Carpathian Keuper) (KkT3)
- Triassic dolomite (dT23)
- Triassic limestone (Gutenstein Fm.) (GvT2)
- Triassic sandstone and shale (Benkovský Fm.) (BeT1)
- Triassic sandstone (Lúžňanská Fm.) (LuT1)
- Other Triassic sediment (LuT3 and pbT1)
- Permian sandstone and conglomerate (mPh)
- Permian basalt (Malužinská Fm.) (vPh)
- Carboniferous clastic sediment (Nižnobocianske Fm.) (sCh)
- Variscan granodiorite (gr7)
- Metamorphic 'basement'

Figure 7

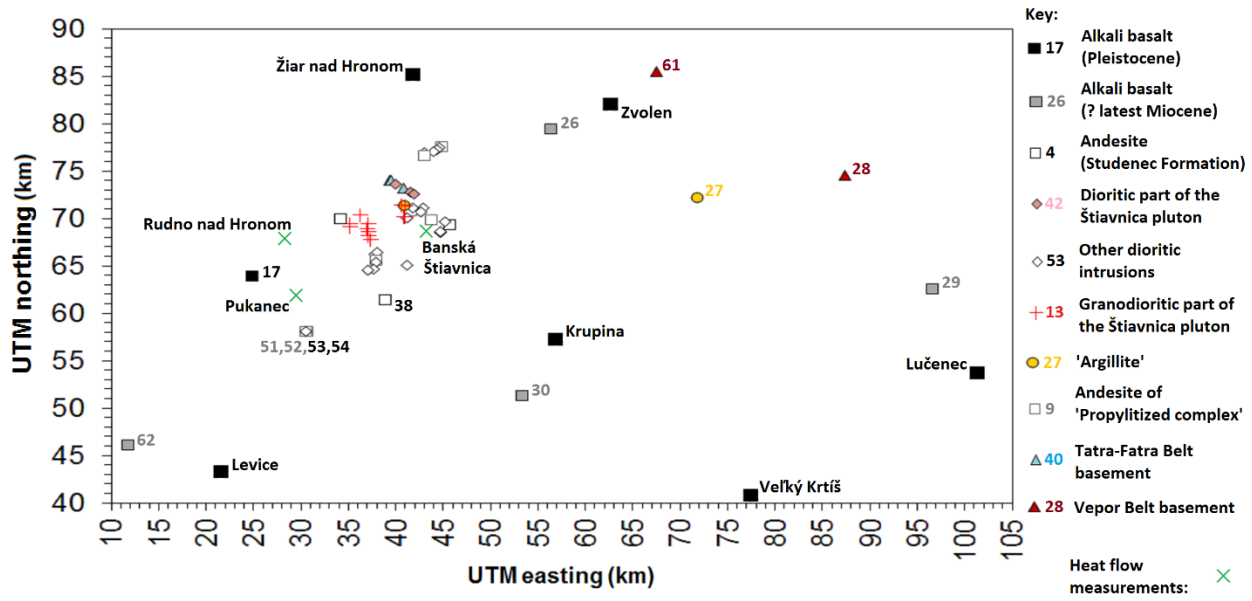
Key:
17 Alkali basalt (Pleistocene)
26 Alkali basalt (? latest Miocene)
4 Andesite (Studenec Formation)
42 Dioritic part of the Štiavnica pluton
53 Other dioritic intrusions
13 Granodioritic part of the Štiavnica pluton
27 'Argillite'
9 Andesite of 'Propylitized complex'
40 Tatra-Fatra Belt basement
28 Vepor Belt basement
Heat flow measurements:
Žiar nad Hronom
Zvolen
Rudno nad Hronom
Banská Štiavnica
Pukanec
Krupina
Lučenec
Levice
Veľký Krtíš
51,52,53,54
UTM northing (km)
UTM easting (km)

(a)

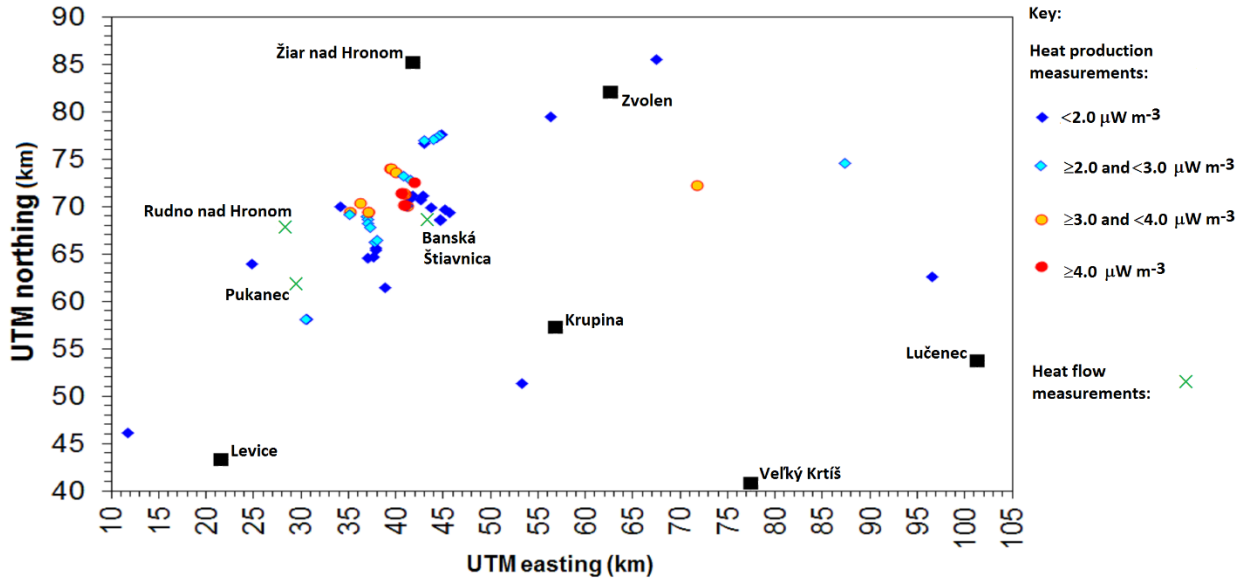
Key:
Heat production measurements:
<2.0 μW m-3
≥2.0 and <3.0 μW m-3
≥3.0 and <4.0 μW m-3
≥4.0 μW m-3
Heat flow measurements:
Žiar nad Hronom
Zvolen
Rudno nad Hronom
Banská Štiavnica
Pukanec
Krupina
Lučenec
Levice
Veľký Krtíš
UTM northing (km)
UTM easting (km)

(b)

Figure 8

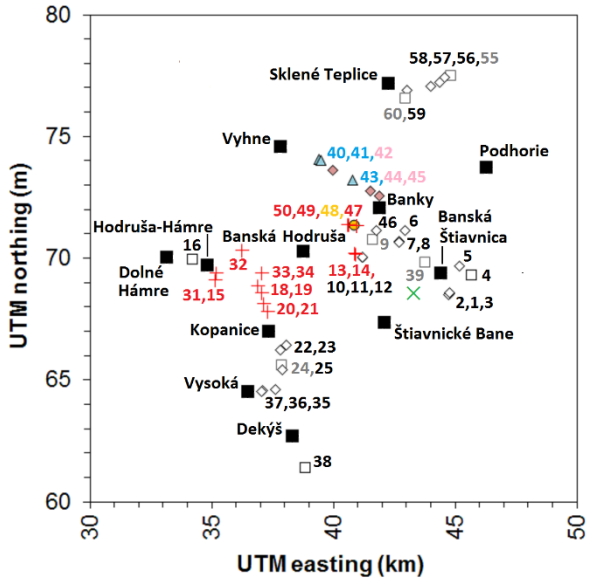
UTM northing (m)
UTM easting (km)
Sklené Teplice
58,57,56,55
60,59
Vyhne
Podhorie
40,41,42
43,44,45
Banky
50,49,48,47
46
6
Banská Štiavnica
Hodruša-Hámre
16
Banská Hodruša
9
7,8
5
Dolné Hámre
32
33,34
13,14,
39
4
31,15
18,19
10,11,12
2,1,3
20,21
Kopanice
Štiavnické Bane
22,23
24,25
Vysoká
37,36,35
Dekýš
38

(a)

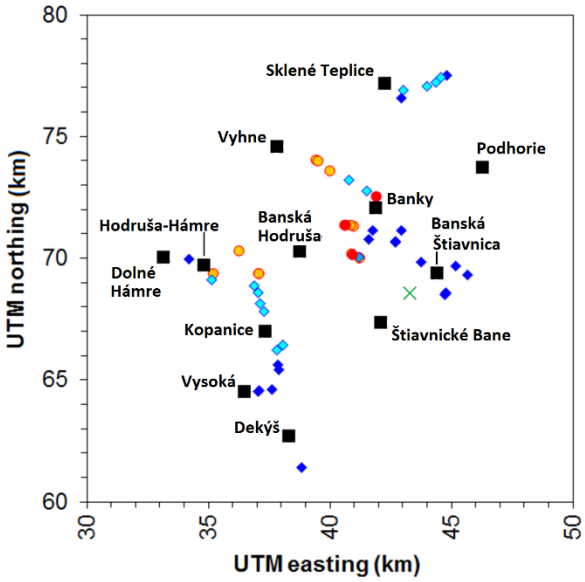
UTM northing (km)
UTM easting (km)
Sklené Teplice
Vyhne
Podhorie
Banky
Hodruša-Hámre
Banská Hodruša
Banská Štiavnica
Dolné Hámre
Kopanice
Štiavnické Bane
Vysoká
Dekýš

(b)

Figure 9

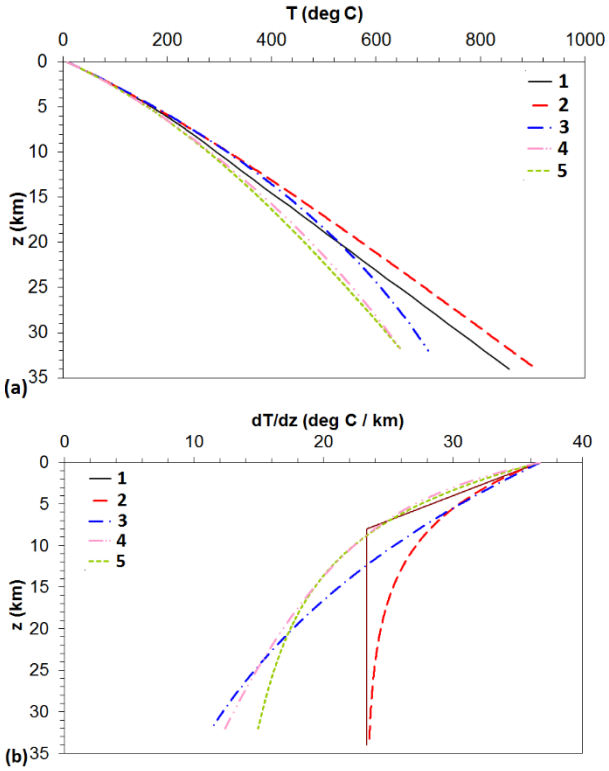
T (deg C)
0
200
400
600
800
1000
z (km)
0
5
10
15
20
25
30
35
1
2
3
4
5
(a)
dT/dz (deg C / km)
0
10
20
30
40
z (km)
0
5
10
15
20
25
30
35
1
2
3
4
5
(b)

Figure 10

Table 1: Heat flow data reported by Čermák (1979)

Site	Locality	UTM / MGRS co-ordinates			Křovák co-ordinates		Note	h	c	k	q	Note	c	k	q	Note
		Quad	east (m)	north (m)	X (m)	Y (m)		(m)	(°C km^{-1})	(W m^{-1} °C^{-1})	(mW m^{-2})		(°C km^{-1})	(W m^{-1} °C^{-1})	(mW m^{-2})	
Borehole D-14	Miková	DU	44758	88635	-337320	-1243631	1	322	16.1	3.86	62.1	4	19.8	3.45	68.3	7
Borehole PO-86	Podhradie	CU	29227	92624	-452523	-1233877	2	824	34.6	2.04	70.6	4	35.2	2.10	74.0	7
Borehole GK-9	Rudno/Hronom	CU	28406	67836	-454582	-1258592	2	239	30.0	2.37	71.0	5	40.5	2.10	85.0	7
Borehole GK-14	Pukanec	CU	29473	61826	-453817	-1264648	2	375	33.6	2.11	71.0	5	36.5	2.68	97.8	7
Borehole KR-3	Kremnicé Bane	CU	46758	99889	-434652	-1227496	2	777	25.0	2.84	71.0	5	29.9	2.78	83.0	7
Borehole KL-2	Kolárovo	BU	78901	12576	-506792	-1311294	1	111	40.1	2.27	91.0	4	43.1	2.01	86.5	7
Klinger Kratka	Banská Štiavnica	CU	43276	68572	-439694	-1258602	3	650	ND	ND	111.0	6	ND	ND	ND	

Unless otherwise stated, data are from Čermák (1979). The heat flow measurement at Banská Štiavnica is from Boldizsár (1964); those at Rudno nad Hronom, Pukanec, and Kremnica are from Lizoň (1975). Universal Transverse Mercator / Military Grid Reference System co-ordinates are in zone 34U.

Notes:

1: The borehole could not be located on the online geological map, so the approximate geographical co-ordinates given by Čermák (1979) were converted to UTM co-ordinates and thence to Křovák co-ordinates.

2: The approximate geographical co-ordinates given by Čermák (1979) were used to locate borehole on online geological map. The Křovák co-ordinates thus indicated were converted to UTM co-ordinates.

3: The approximate geographical co-ordinates given by Čermák (1979) were used to locate the vicinity on Google Earth. The UTM co-ordinates thus indicated for the entrance to Klinger Kratka Mine were converted to Křovák co-ordinates.

4: Heat flow q has been calculated (as c × k) from values of c and k reported by Čermák (1979). Čermák (1979) determined different values for heat flow, respectively 70.0, 68.7 and 75.0 mW m^{-2} for boreholes D-14, PO-86, and KL-2. For boreholes D-14 and PO-86 the cause of these discrepancies appears to relate to the calculation of topographic corrections (cf. Čermák, 1977).

5: Heat flow q and the geothermal gradient c were reported by Čermák (1979), from which thermal conductivity k has been calculated (as q / c).

6: Boldizsár (1964) and Čermák (1979) only reported the heat flow q, not corresponding values of c or k, which are therefore not determined (ND).

7: Values of c, k and q reported by or derived from Franko et al. (1995). Note that these differ from the corresponding values from Čermák (1979); we cannot explain these discrepancies.

Table 2: Borehole geothermal data from Franko et al. (1995)

No.	ID	Locality	Latitude	Longitude	T_{500} (°C)	T_{1000} (°C)	T_{1500} (°C)	T_{2000} (°C)	q (mW m^{-2})	k (W m^{-1} °C^{-1})
Resurgent horst										
4	B-1	Horná Roveň	48°26’48”	18°51’46”	23	38	56	69	(83.6)	(3.00)
96	HDŠ-3	Voznica	48°27’19”	18°46’34”	26	39	51		(85.6)	(3.00)
97	HDŠ-4	Kopanice	48°25’56”	18°48’56”	26	38			(89.5)	(3.00)
98	HDŠ-5	Banská Štiavnica	48°28’08”	18°52’05”	29	48			(114.0)	(3.00)
99	HDŠ-6	Hodruša	48°27’32”	18°48’21”	26	43	59		(99.0)	(3.00)
100	HDV-1	Hodruša	48°27’28”	18°46’52”	27	46			(114.0)	(3.00)
101	HDV-7	Hodruša	48°28’06”	18°49’33”	25	42			(102.0)	(3.00)
102	HDV-9	Hodruša	48°28’37”	18°48’36”	20	36			(96.0)	(3.00)
103	HDV-10	Hodruša	48°29’04”	18°49’48”	20	34			(84.0)	(3.00)
104	HDV-12	Repište	48°29’52”	18°50’22”	26	44			(108.0)	(3.00)
105	HDV-13	Hodruša	48°27’34”	18°50’14”	28	46			(108.0)	(3.00)
106	HDV-15	Hodruša	48°28’49”	18°52’12”	21				(76.8)	(3.00)
117	JB-10	Vyhne	48°28’55”	18°49’53”	22				(82.8)	(3.00)
125	KOV-39	Štiavnicé Bane	48°26’02”	18°51’43”	26	43	55		(87.0)	(3.00)
126	KOV-40	Podsitnianska	48°26’09”	18°52’54”	26	39			(78.0)	(3.00)
127	KOV-41	Podhorie	48°29’11”	18°54’30”	23	34			(77.4)	(3.00)
128	KOV-42	Banská Štiavnica	48°27’30”	18°54’40”	25	41			(96.0)	(3.00)
129	KOV-43	Banská Štiavnica	48°29’26”	18°53’43”	21	34			(78.0)	(3.00)
130	KOV-44	Banská Štiavnica	48°28’49”	18°55’17”	25	37			(86.4)	(3.00)
174	MI-1	Banská Štiavnica	48°27’29”	18°54’08”	29	49			(120.0)	(3.00)
175	MI-3	Banská Štiavnica	48°27’52”	18°54’00”	29	47			(108.0)	(3.00)
203	R-1	Zlatno	48°25’42”	18°46’28”	30	44			(107.4)	(3.00)
204	R-2	Zlatno	48°25’41”	18°45’58”	26	50			(125.4)	(3.00)
205	R-4	Zlatno	48°25’43”	18°46’48”	23	40			103.3	[3.04]
206	R-6	Zlatno	48°25’20”	18°46’44”	25	40			100.2	[3.34]
207	R-7	Zlatno	48°25’25”	18°46’23”	26	43			(102.0)	(3.00)
208	R-8	Zlatno	48°25’18”	18°46’24”	26				(106.8)	(3.00)
209	R-9	Zlatno	48°25’26”	18°46’43”	29	47			104.6	[2.91]
210	R-10	Zlatno	48°25’00”	18°47’18”	24	38	52		(84.0)	(3.00)
211	R-11	Zlatno	48°25’13”	18°46’35”	26	42			96.2	[3.01]
212	R-12	Zlatno	48°25’26”	18°46’43”	29	47			(108.0)	(3.00)
213	R-13	Zlatno	48°25’21”	18°46’54”	27	44			(102.0)	(3.00)
214	R-15	Zlatno	48°25’24”	18°46’04”	25	45			(120.0)	(3.00)
215	R-16	Zlatno	48°25’33”	18°46’41”	25	43			(104.4)	(3.00)
216	R-17	Zlatno	48°25’31”	18°46’22”	22	37			(90.0)	(3.00)
217	R-18	Zlatno	48°25’17”	18°46’15”	24	39			(90.0)	(3.00)
218	R-20	Zlatno	48°25’24”	18°46’14”	22	32			(71.4)	(3.00)
219	R-21	Zlatno	48°25’15”	18°46’55”	24	38			(89.4)	(3.00)
220	R-23	Zlatno	48°25’16”	18°46’04”	24	42			(101.4)	(3.00)
221	R-24	Zlatno	48°25’11”	18°46’26”	21	35			(80.4)	(3.00)
222	R-25	Zlatno	48°25’23”	18°46’38”	26	42			(101.4)	(3.00)
269	SSH-2	Podhorie	48°29’30”	18°55’12”	27				108.0	[2.87]
271	ST-5	Sklené Teplice	48°31’38”	18°53’05”	28				(118.8)	(3.00)
278	ŠB-1	Štiavnické Bane	48°26’20”	18°51’22”	28	44			(107.4)	(3.00)
279	ŠB-3	Štiavnické Bane	48°25’47”	18°52’10”	23	40			(102.0)	(3.00)
280	ŠB-4	Rychnava	48°25’55”	18°50’57”	22	39			(102.0)	(3.00)
284	ŠPZ-1	Banská Štiavnica-Piarg	48°25’55”	18°52’32”	23	39			(96.0)	(3.00)
307	UB-1	Uhliská	48°24’19”	18°46’12”	35	53			(108.0)	(3.00)
322	VNOŠ-1	Hodruša	48°26’54”	18°46’13”	30				(130.8)	(3.00)
323	VNOŠ-2	Hodruša	48°26’59”	18°49’43”	25				(100.8)	(3.00)
332	VŠ-6	Štiavnické Bane	48°26’46”	18°52’49”	22	38			(96.0)	(3.00)

Caldera and surroundings

5	BB-21	Ilija	48°25’05”	18°54’34”	37				(126.7)	(2.20)
23	BT-7	Pukanec	48°20’58”	18°42’06”	25	43			(76.6)	(2.20)
67	GK-2	Antol	48°24’46”	18°56’24”	37	60			(101.2)	(2.20)
74	GK-9	Rudno nad Hronom	48°26’25”	18°40’55”	30	54	69		85.0	[2.18]
76	GK-12	Devičany	48°20’08”	18°40’43”	29	38			(65.6)	(2.20)
77	GK-13	Nová Baňa	48°25’49”	18°38’58”	34	53	72		(83.6)	(2.20)
78	GK-14	Brehy	48°23’09”	18°41’00”	32	49	63		97.8	[3.15]
79	GK-15	Brehy	48°23’25”	18°41’03”	34	54	70		(79.2)	(2.20)
94	HDŠ-1	Repište	48°30’54”	18°49’54”	27				(82.7)	(2.20)
95	HDŠ-2	Dolné Hámre-Kyslá	48°27’53”	18°45’25”	30	47			(74.8)	(2.20)
107	HF-1	Hliník nad Hronom	48°32’36”	18°50’05”	32	54			(96.8)	(2.20)
119	JP-1	Jastrabá	48°37’49”	18°56’55”	41	59			(79.2)	(2.20)
157	LKC-1	Banská Štiavnica	48°27’00”	18°55’48”	31	50	68	86	(80.7)	(2.20)
172	MEB-1	Prochot	48°36’42”	18°42’05”	29	49			(88.0)	(2.20)
189	P-8	Rudno-Chlm	48°24’26”	18°40’52”	30	49			(83.6)	(2.20)
270	ST-4	Sklené Teplice	48°32’33”	18°50’33”	32	50	66		(74.8)	(2.20)
337	VTV-21	Vtáčnik	48°35’49”	18°40’30”	29	45			(70.4)	(2.20)

Geothermal data from boreholes within ~20 km of the Štiavnica Pluton, from Franko et al. (1995). Borehole numbers show locations in Fig. 5(b). IDs are unique identifiers for each borehole within Slovakia. T_{500}, T_{1000}, T_{1500} and T_{2000} indicate temperatures at depths of 500, 1000, 1500 and 2000 m where reported. Heat flow q and thermal conductivity k are determined as follows. Values of q not inside brackets are from Franko et al. (1995); they are consistent with the values of k inside square brackets, reported in the present study. Values of q inside round brackets are estimated in the present study using the nominal values of k inside round brackets, which are set to 3.00 W m^{-1} $°C^{-1}$ to represent the granitic rocks in the resurgent horst and 2.20 W m^{-1} $°C^{-1}$ to represent the andesites in the surrounding caldera. Calculations relate to the temperature intervals indicated or to nominal surface temperatures of 8.2 °C, based on meteorological data from Banská Štiavnica (from https://en.climate-data.org/location/208/).

Table 3: Gamma-ray spectrometry measurements

S	Co-ordinates UTM		Křovák		Location	Map symbol	N	Interpret-ation	P	Lithology	K wt% (±1σ)		U ppm (±1σ)		Th ppm (±1σ)		Y μW m^{-3} (±1σ)	
Post-orogenic basalts																		
17	24898	63925	-458281	-1262323	Brehy	Oc01Q1		Alkali basalt	6	Alkali basalt (lava), Pleistocene	1.78	0.18	2.73	0.23	9.12	0.94	1.50	0.03
26	56364	79447	-426078	-1248394	Ostrá Lúka	Oc0Pt		Alkali basalt	6	Alkali basalt (lava), 'Pontian'	1.06	0.13	1.89	0.14	10.12	0.60	1.29	0.04
29	96534	62592	-386796	-1267238	Podrečany	Oc0Pt		Alkali basalt	6	Alkali basalt (lava), 'Pontian'	1.67	0.14	2.12	0.98	6.03	0.95	1.12	0.18
30	53273	51277	-430574	-1276376	Rakovec	Oc0Pt		Alkali basalt	6	Alkali basalt (lava), 'Pontian'	1.41	0.19	1.29	0.82	8.67	1.67	1.06	0.11
62	11708	46125	-472345	-1279439	Mochovce	Oc0Pt		Alkali basalt	6	Alkali basalt (lava), 'Pontian'	2.11	0.11	2.82	0.64	11.01	1.36	1.68	0.07
											1.60		2.17		8.99		1.33	
Granodioritic part of the Štiavnica pluton																		
13	40893	70192	-441993	-1256864	Below Hodrušské Jazero reservoir	Si8BS		HSIC	2	Granodiorite (pluton)	8.99	0.37	5.62	0.80	11.21	2.27	3.06	0.07
14	40932	70171	-441955	-1256887	Below Hodrušské Jazero reservoir	Si8BS		HSIC	2	Granodiorite (pluton)	7.70	0.47	8.11	0.91	18.63	2.11	4.10	0.36
15	35163	69396	-447755	-1257373	Hodruša-Hámre	Si8BS		HSIC	2	Granodiorite (pluton)	5.56	0.12	4.21	0.54	24.00	0.50	3.26	0.11
18	36904	68875	-446043	-1257980	North of Kopanice	Si8BS		HSIC	2	Granodiorite (pluton)	5.39	0.15	2.97	1.02	17.05	2.53	2.45	0.11
19	37043	68594	-445918	-1258268	North of Kopanice	Si8BS		HSIC	2	Granodiorite (pluton)	4.65	0.23	3.56	1.00	19.26	2.91	2.68	0.34
20	37119	68152	-445864	-1258713	North of Kopanice	Si8BS		HSIC	2	Granodiorite (pluton)	4.50	0.13	3.57	0.63	21.54	1.85	2.83	0.18
21	37301	67796	-445700	-1259078	North of Kopanice	Si8BS	[1]	HSIC	2	Altered granodiorite (pluton)	3.22	0.06	5.47	0.69	16.94	1.59	2.88	0.07
31	35146	69091	-447788	-1257677	South of Hodruša-Hámre	Si8BS		HSIC	2	Granodiorite (pluton)	6.32	0.26	1.97	0.80	15.88	1.26	2.20	0.26
32	36221	70336	-446652	-1256487	North of Hodruša-Hámre	Si8BS		HSIC	2	Granodiorite (pluton)	8.40	0.34	6.59	1.33	18.16	3.30	3.74	0.28
33	37063	69409	-445857	-1257455	North of Hodruša-Hámre	Si8BS		HSIC	2	Granodiorite (pluton)	5.00	0.02	4.26	0.75	22.48	2.53	3.12	0.25
34	37070	69411	-445850	-1257453	North of Hodruša-Hámre	Si8BS		HSIC	2	Granodiorite (pluton)	5.67	0.16	5.89	0.95	27.76	1.54	3.97	0.26
47	40952	71339	-441876	-1255722	Mountain bike trail west of Hadová	Si8BS		HSIC	2	Highly altered granodiorite (pluton)	7.16	0.09	6.18	0.60	18.55	1.03	3.54	0.09
48	40848	71373	-441979	-1255683	Mountain bike trail west of Hadová	m3		HSIC	2	'Argillite' within granodiorite (pluton)	4.19	0.42	6.52	1.53	15.74	1.02	3.16	0.31
49	40619	71392	-442206	-1255652	Mountain bike trail west of Hadová	Si8BS		HSIC	2	Granodiorite (pluton)	6.29	0.43	8.42	0.70	21.81	1.97	4.27	0.13
50	40604	71398	-442221	-1255645	Mountain bike trail west of Hadová	Si8BS		HSIC	2	Granodiorite (pluton)	7.22	0.30	10.78	0.77	21.27	0.17	4.92	0.18
											6.02		5.61		19.35		3.35	
Dioritic part of the Štiavnica pluton																		
42	39985	73595	-442729	-1253420	SE of Vyhne, NW of Banky	Si9BS	[2]	HSIC	2	Diorite (pluton)	6.78	0.37	6.36	0.78	18.41	0.82	3.54	0.17
44	41512	72761	-441246	-1254329	SE of Vyhne, NW of Banky	Si9BS		HSIC	2	Diorite (pluton)	2.26	0.30	3.87	1.41	12.26	0.55	2.06	0.35
45	41910	72569	-440858	-1254541	Banky	Si9BS		HSIC	2	Diorite (pluton)	4.53	0.10	7.58	0.40	28.85	2.09	4.37	0.04
											4.52		5.94		19.84		3.32	
West of Hodruša-Hámre																		
16	34200	69977	-448688	-1256744	Western end of Hodruša-Hámre	Cd41B3		Studenec Fm	3	Porphyritic andesite (? lava)	1.69	0.15	2.52	0.67	11.54	2.51	1.61	0.01
							[3]				2.30		3.03		14.68		2.01	

Area east of Sklené Teplice																		
55	44829	77503	-437696	-1249759	East of Sklené Teplice	Oa34B23	PC	1	Andesite (lava)	3.04	0.04	3.26	1.35	11.23	0.88	1.90	0.32
56	44590	77435	-437938	-1249815	East of Sklené Teplice	Ci87BS	Banisko IC	2	Highly alt. porphyritic andesite (? sill)	3.09	0.07	3.86	0.31	12.75	1.53	2.16	0.15
57	44353	77227	-438185	-1250011	East of Sklené Teplice	Ci87BS	Banisko IC	2	Kaolinized porphyry (? sill)	2.49	0.06	3.78	0.74	14.58	0.50	2.21	0.16
58	44023	77056	-438523	-1250165	East of Sklené Teplice	Bi84BS	Zlatno IC	2	Alt. porph. and. (? sill) / diorite (?stock)	2.98	0.14	4.78	2.03	15.37	2.00	2.57	0.42
59	43021	76907	-439532	-1250264	East of Sklené Teplice	Bi84BS	Zlatno IC	2	Argillite (altered ? diorite)	2.60	0.15	4.35	0.98	16.45	1.82	2.50	0.18
60	42967	76570	-439602	-1250598	East of Sklené Teplice	Ca29B23	PC	1	Porphyritic (? basaltic) and. (? sill)	1.91	0.21	3.10	0.81	13.15	1.70	1.89	0.08
										2.68		3.86		13.92		2.21	
Hadová area																		
6	42950	71124	-439891	-1256036	Beside Štiavnivké Jazero res. S of Banky	Ci85BS	Banisko IC	2	Porphyritic andesite (sill)	3.83	0.33	4.71	1.84	15.46	1.19	2.64	0.37
7	42699	70680	-440165	-1256467	Hadová turnoff, north of road	Ci87BS	Banisko IC	2	Kaolinized porphyritic and. (sill)	2.63	0.34	4.82	1.21	14.95	0.69	2.52	0.29
8	42714	70662	-440150	-1256486	Hadová turnoff, south of road	Ci87BS	Banisko IC	2	Kaolinized porphyritic and. (sill)	3.75	0.13	4.47	0.46	17.86	1.44	2.74	0.10
9	41616	70770	-441242	-1256323	On road east of Hodruša-Hámre	Oa28B23	PC	1	Porphyritic andesite (lava)	2.47	0.26	3.49	1.18	10.68	1.77	1.87	0.20
46	41782	71132	-441058	-1255970	East of Hadová	Ci87BS	Banisko IC	2	Porphyritic andesite (sill)	2.52	0.25	3.31	1.13	10.97	0.64	1.85	0.26
										3.18		4.32		14.81		2.43	
Banská Štiavnica area																		
1	44757	68549	-438466	-1263692	SW of Banská Štiavnica; highway 524	Ci87BS	Banisko IC	2	Porphyritic andesite (? sill)	4.16	0.18	2.60	1.35	15.67	1.38	2.14	0.26
2	44752	68507	-438223	-1258740	SW of Banská Štiavnica; highway 524	Ci87BS	Banisko IC	2	Porphyritic andesite (? sill)	3.35	0.18	2.24	0.11	11.58	0.96	1.69	0.09
3	44765	68594	-438205	-1258654	SW of Banská Štiavnica; highway 524	Ci87BS	Banisko IC	2	Porphyritic andesite (? sill)	4.49	0.31	2.64	0.90	17.07	1.81	2.28	0.11
4	45691	69302	-437245	-1257993	East of Banská Štiavnica on highway 525	Od5B3	Studenec Fm	3	Porphyritic andesite (lava)	3.20	0.32	3.68	1.97	17.84	1.22	2.48	0.40
5	45177	69683	-437739	-1257587	NE of Banská Štiavnica near highway 525	Ci87BS	Banisko IC	2	Porphyritic andesite (? sill)	1.64	0.11	2.79	0.42	9.89	1.59	1.56	0.18
39	43747	69854	-439159	-1257345	North of Banská Štiavnica	Ca29B23	PC	1	Porphyritic andesite (? sill)	3.46	0.06	2.56	0.39	9.63	0.73	1.65	0.09
Area adjoining the Hodrušské Jazero reservoir																		
10	41192	70042	-441702	-1257029	Beside Hodrušské Jazero reservoir	Ci85BS	Banisko IC	2	Kaolinized andesite (sill)	3.85	0.22	6.12	0.32	20.17	0.96	3.33	0.09
11	41204	70031	-441690	-1257041	Beside Hodrušské Jazero reservoir	Ci85BS	Banisko IC	2	Kaolinized andesite (sill)	2.71	0.31	4.67	1.14	15.07	1.82	2.50	0.19
12	41215	70022	-441680	-1257050	Beside Hodrušské Jazero reservoir	Ci85BS	Banisko IC	2	Kaolinized andesite (sill)	3.00	0.16	3.52	0.25	15.22	0.74	2.24	0.11
										3.01		4.45		15.29		2.48	
Kopanice area																		
22	37807	66245	-445272	-1260652	South of Kopanice	Ci84BS	Banisko IC	2	Porphyritic andesite (sill)	2.79	0.68	3.37	1.95	13.45	0.93	2.06	0.38
23	38065	66441	-445005	-1260469	Eastern edge of Kopanice	Ci84BS	Banisko IC	2	Porphyritic andesite (sill)	2.79	0.03	4.69	0.14	15.09	1.53	2.51	0.14
24	37877	65601	-445235	-1261299	On rough road south of Kopanice	Oa28B23	PC	1	Aphyric andesite (lava)	2.40	0.40	1.70	1.04	11.00	0.17	1.42	0.29
25	37922	65409	-445199	-1261493	On rough road south of Kopanice	Ci85BS	Banisko IC	2	Argillite / highly altered and. (? sill)	8.26	0.40	1.30	1.08	7.61	1.57	1.64	0.34
										4.06		2.77		11.79		1.91	

Vysoká area																		
35	37641	64615	-445520	-1262272	East of Vysoká	Bi83BS	Banisko IC	2	Argillite / highly altered and. (? sill)	2.96	0.11	1.38	1.18	10.77	1.03	1.38	0.23
36	37089	64549	-446074	-1262310	Vysoká	Ci89BS	Banisko IC	2	Altered porphyritic and. (? sill)	1.74	0.11	2.07	1.50	10.39	0.28	1.42	0.37
37	37033	64517	-446132	-1262339	Vysoká	Ci89BS	Banisko IC	2	Porphyritic andesite (? sill)	1.63	0.13	2.91	1.49	10.52	1.57	1.63	0.27
38	38859	61408	-444464	-1265536	Dekýš	Od42B3	Studenec Fm	3	Porphyritic andesite (lava)	2.02	0.62	2.89	0.73	14.66	2.50	1.95	0.17
										2.09		2.31		11.59		1.59	
Pukanec area																		
51	30675	58050	-452805	-1268480	Pukanec	Aa2B2	EC	1	Porphyritic andesite (? lava)	5.31	0.13	0.37	0.61	6.92	0.34	1.07	0.16
52	30503	58115	-452974	-1268406	Pukanec	Aa2B2	EC	1	Argillitized andesite (? lava)	4.02	0.13	1.77	0.38	8.64	0.74	1.43	0.13
53	30561	58040	-452920	-1268484	Pukanec	Bi85BS	Tatiar IC	2	Porph. and. (? sill) / diorite (?stock)	4.65	0.10	2.76	0.86	12.22	1.96	1.99	0.09
54	30580	58042	-452901	-1268483	Pukanec	Bi85BS	Tatiar IC	2	Porph. and. (? sill) / diorite (?stock)	4.43	0.40	2.80	0.45	10.91	0.74	1.89	0.08
										4.60		1.93		9.67		1.60	
Javorie 'argillite'																		
27	71755	72189	-411068	-1256413	Vigľašská Huta - Kalinka	m3	ND	2	'Argillite' (? pluton)	3.57	0.40	6.16	1.77	18.40	2.05	3.19	0.41
Vepor Belt basement																		
28	87351	74574	-395370	-1254810	Podkriváň	gr23	'pre Tertiary'	0	Granodiorite	2.77	0.04	2.65	0.43	16.95	1.51	2.11	0.14
61	67527	85424	-414629	-1242982	Lieskovec	gr23	'pre Tertiary'	0	Granodiorite	3.44	0.09	1.85	0.68	7.72	0.62	1.33	0.21
										3.11		2.25		12.34		1.72	
Tatra-Fatra Belt basement																		
40	39403	74046	-443288	-1252941	SE of Vyhne, NW of Banky	gr7	'pre Tertiary'	0	Granitic schist	6.58	0.16	5.36	1.47	16.97	2.67	3.17	0.24
41	39484	74029	-443208	-1252962	SE of Vyhne, NW of Banky	gr7	'pre Tertiary'	0	Granitic schist	6.76	0.23	5.07	0.94	23.59	0.98	3.57	0.28
43	40798	73220	-441936	-1253836	SE of Vyhne, NW of Banky	gr7	'pre Tertiary'	0	Granitic schist	5.34	0.11	3.43	0.59	19.73	1.79	2.75	0.08
										6.23		4.62		20.09		3.16	

S indicates measurement number; Co-ordinates are given in both UTM (zone 34U; quadrangle CU) and Křovák systems; 'Map symbol' denotes the code used to denote this lithology on the online geological map; N denotes any notes relating to these map symbols or other information in each row of the Table; 'Interpretation' denotes the classification by Chernyshev et al. (2013); P denotes the phase of magmatism to which the rock at the site is assigned (cf. Fig. 2, with ND denoting 'not determined'); Lithology denotes our classification of the lithology at each site (alt. denotes hydrothermally altered or 'propylitized'; and. denotes andesite; porph. denotes porphyritic); K, U and Th denote the concentrations of the three heat-producing elements and their associated margins of uncertainty; and Y denotes the associated heat production, calculated using equation (1), with its margin of uncertainty. Each of the groupings of more than one site is followed by a row containing mean values of K, U, Th and Y.

In the 'Map symbol' column, most outcrops are assigned a code in which the last group of symbols denotes the estimated age of the unit (B2, Middle Badenian; B23, Middle-Late Badenian; B3, Late Badenian; BS Badenian/Sarmatian; Pt, Pontian; Q1, Early Quaternary). Some of these age assignments are now known to be incorrect, as is discussed in the text. These age codes are preceded by letters and digits: the letters are an abbreviation of a word in Slovak describing the lithology, the digits set out to distinguish between the different units of this type that have been recognized. The geological map indeed shows a vast proliferation of marginally different classifications, many of which (we argue) might well indicate compositional zonation within the same igneous bodies. A different system is used on the map for classifying basement rocks and 'argillite'. In the column listing how Chernyshev et al. (2013) designated the various lithologies, IC denotes 'igneous complex', EC denotes their 'Effusive complex'; HSIC denotes their 'Hodruša-Štiavnica igneous complex'; and PC their 'Propylitized complex'.

Notes:

[1] The geological map indicates lithology Ci85BS, meaning andesite, at this site; the outcrop and rock sample collected from it are clearly of granodiorite (lithology Si8BS).

[2] The geological map indicates lithology BeT1, meaning sandstone and mudstone of the Early Triassic Benkov Formation at this site; the outcrop and rock sample collected are clearly of diorite (lithology Si9BS).

[3] This set of mean values is for the three sites that are grouped, according to Chernyshev et al. (2013), within the Studenec Formation.